RSC Advances

This is an *Accepted Manuscript*, which has been through the Royal Society of Chemistry peer review process and has been accepted for publication.

Accepted Manuscripts are published online shortly after acceptance, before technical editing, formatting and proof reading. Using this free service, authors can make their results available to the community, in citable form, before we publish the edited article. This *Accepted Manuscript* will be replaced by the edited, formatted and paginated article as soon as this is available.

You can find more information about *Accepted Manuscripts* in the Information for Authors.

Please note that technical editing may introduce minor changes to the text and/or graphics, which may alter content. The journal's standard Terms & Conditions and the Ethical guidelines still apply. In no event shall the Royal Society of Chemistry be held responsible for any errors or omissions in this *Accepted Manuscript* or any consequences arising from the use of any information it contains.

ROYAL SOCIETY OF CHEMISTRY

www.rsc.org/advances

A series of coordination polymers based on varied polycarboxylates and different imidazole-containing ligands: Syntheses, crystal structures and physical properties

Xiao-Feng Wang[a], **Min Yu**[a], **and Guang-Xiang Liu**[a,b,*]

[a] *Key Laboratory of Advanced Functional Materials of Nanjing, Department of Chemistry, Nanjing Xiaozhuang University, Nanjing 211171, P. R. China*

[b] *State Key Laboratory of Coordination Chemistry, School of Chemistry and Chemical Engineering, Nanjing University, Nanjing 210093, P. R. China*

Corresponding Author:

Dr. Guang-Xiang Liu

Mailing Address: *Key Laboratory of Advanced Functional Materials of Nanjing, Nanjing Xiaozhuang University, Nanjing 211171, P. R. China*

Telephone: *+86-25-86178131*

Fax: *+86-25-8617222*

E-mail: *njuliugx@126.com (G. X. Liu)*

RSC Advances Accepted Manuscript

Abstract

To investigate the effect of organic ligands on the coordination frameworks, seven new nickel complexes with formulae Ni(BDC)(titmb)·3H_2O (**1**), $Ni_2(BDC)_2(bimb)_2(H_2O)_2$·3$H_2O$ (**2**), NiZn(BTC)(titmb)Br (**3**), Ni(TBDC)(titmb)(H_2O) (**4**), Ni(TBDC)(bix)·H_2O (**5**), Ni(TBDC)(mbix)(H_2O)·H_2O (**6**) and Ni(TBDC)(obix)(H_2O) (**7**) (titmb = 1,3,5-tris(1-imidazol-1-ylmethyl)-2,4,6-tri-methylbenzene, bimb = 4,4'-bis(imidazol-1-ylmethyl)biphenyl, bix = 1,4-bis(imidazol-1-ylmethyl)benzene, mbix = 1,3-bis(imidazol-1-ylmethyl)benzene, obix = 1,2-bis(imidazol-1-ylmethyl)benzene, H_3BTC = 1,3,5-benzenetricarboxylic acid, H_2BDC = isophthalic acid, H_2TBDC = 5-(tertbutyl)isophthalic acid), have been synthesized and characterized by elemental analyses, infrared spectra (IR), thermogravimetric analyses (TGA) and single-crystal X-ray diffraction. Single crystal structure analysis shows that complex **1** shows a three-dimensional (3D) (3,5)-connected network with the topology of $(6^3)(6^9.8)$. Complexes **2** and **6** have similar two-dimensional (2D) lamella structure with (4,4) topology. Complex **3** exhibits an interesting 3D (3,6)-connected framework by self-penetration of two sets of (10,3)-a nets. Complex **4** presents a unusual 2D (3,5)-connected framework with the topology of $(3.5^2)(3^2.5^3.6^4.7)$. Complex **5** features a 3D two-fold interpenetrating framework with $(4^6.6^4)$-**bnn** hexagonal BN topology, whereas Complex **7** possesses an interesting one-dimensional (1D) independent single-wall metal-organic nanotube. The various dimensions and structural features of seven complexes may be attributed to the different species of functional groups, the number and position of the carboxylic groups in the carboxylates as well as the auxiliary ligands play a

RSC Advances Accepted Manuscript

significant role in promoting the diversity of the observed structural motifs. The SHG properties of **1**, **3** and **4** as well as ferroelectric properties for **1** have also been investigated.

Keywords: Nickel(II) coordination polymer; polycarboxylate; imidazole-containing ligands; nonlinear optical property; ferroelectric property

Introduction

Rational design and synthesis of coordination polymers (CPs) with tailor-made structures have been one of the most attractive areas in crystal engineering and supramolecular chemistry, because coordination polymers with desired structures possess interesting functionalities and can act as potential materials in the field of gas storage and separation, magnetism, catalysis, non-linear optics, luminescence and ion exchange.[1-6] In the realm of CPs, structure control is fundamental for determining the properties and applications of the crystalline materials. Accordingly, numerous intriguing structures and associated interesting properties have been investigated in depth.[7-8] Though great progress and developments have been made in the construction of diverse architectures, the prediction of the precise solid-state structures or the control of structural dimensionality of CPs remains a long-term challenge in the field of crystal engineering.[9] Many factors affect the structural assembly process of the CPs, such as the metal, the ligand, temperature, pH value of the reaction, the solvent, the counter anions, and the ratio of ligand and metal.[10-15] It has been established that the

RSC Advances Accepted Manuscript

ligands are crucial for the structural architectures and functionalities of CPs as the structures and properties of these complexes are usually influenced by the flexibility, shape, symmetry, length and substituent groups of ligands.[16]

Polycarboxylates are often used as bridging ligands to prepare CPs due to their versatile coordination modes, high structural stability and the ability to balance the positive charges.[17] Moreover, in view of the previous reports, it is found that angular dicarboxylates (isophthalic acid) and its derivatives (5-nitroisophthalic acid) may have an influence on the assembling processes, the structures and even the properties of CPs due to their geometric and electronic effects, while the use of the large hindrance of the derivatives of the dicarboxylate remains largely unexplored. To the best of our knowledge, there have been only a few reported coordination polymers based on the H_2TBDC ligand.[18] As is well known, the mixed ligand strategy added the scope of the CPs, giving diversified polymeric structures with interesting structures and unusual properties.[19] In this regard, bridging imidazole ligands have chance to find their niche in the crystal engineering. Up to now, the bis(imidazole) ligands have been justified as an efficient and versatile organic building unit for construction of coordination polymers by Cui and Zheng et al. groups;[20] however, we believe that the CPs of these ligands with varied structures and topologies could still be achieved by changing assembly environments and strategies. As continuous exploration on the study of Ni(II)-CPs with angular dicarboxylate and different imidazole-containing ligands, seven nickel coordination polymers, namely, Ni(BDC)(titmb)·3H_2O (**1**), $Ni_2(BDC)_2(bimb)_2(H_2O)_2$·3$H_2O$ (**2**), NiZn(BTC)(titmb)Br (**3**), Ni(TBDC)(titmb)(H_2O)

RSC Advances Accepted Manuscript

(**4**), Ni(TBDC)(bix)·H_2O (**5**), Ni(TBDC)(mbix)(H_2O)·H_2O (**6**) and Ni(TBDC)(obix)(H_2O) (**7**), have been successfully obtained. They are characterized by elemental analysis and X-ray crystallography. The crystal structures as well as topological analysis of these complexes will be represented and discussed in detail. In addition, their physical properties are also studied.

Experimental section

Materials and general methods

All the reagents and solvents for syntheses and analyses were purchased from Sigma or TCI and employed as received without further purification. The titmb, bimb, bix, mbix and obix ligands were prepared according to the reported method.[21] Elemental analyses (C, H and N) were performed on a Vario EL III elemental analyzer. Infrared spectra were performed on a Nicolet AVATAR-360 spectrophotometer with KBr pellets in the 4000 - 400 cm^{-1} region. Thermal gravimetric analyses (TGA) were performed on a Netzsch STA-409PC instrument in flowing N_2 with a heating rate of 10 ºC min^{-1}. The second-order nonlinear optical intensity was estimated by measuring a powder sample relative to urea. A pulsed Q-switched Nd:YAG laser at a wavelength of 1064 nm was used to generate a SHG signal from powder samples. The backscattered SHG light was collected by a spherical concave mirror and passed through a filter that transmits only 532 nm radiation. The ferroelectric property of the solid-state sample was measured by the Premier II ferroelectric tester at room temperature.

Preparation of Ni(BDC)(titmb)·$3H_2O$ (1). A mixture containing $Ni(NO_3)_2·6H_2O$

RSC Advances Accepted Manuscript

(58.2 mg, 0.2 mmol), H_2BDC (19.3 mg, 0.1 mmol), titmb (36.0 mg, 0.1 mmol) and $LiOH·H_2O$ (8.4 mg, 0.2 mmol) in 15 ml deionized water was sealed in a 25 mL Teflon lined stainless steel container and heated at 140 ºC for 3 days. Green block crystals of **1** were collected by filtration and washed with water and ethanol several times with a yield of 71%. Anal. calcd for $C_{29}H_{34}N_6O_7Ni$: C 54.65; H 5.38; N 13.19; Found: C 54.66; H 4.36; N 13.17%. IR(KBr pellet, cm^{-1}): 3459 (br), 3057 (w), 2923 (w), 1607 (s), 1541 (s), 1520 (m), 1444 (w), 1432 (m), 1382 (s), 1282 (w), 1233 (m), 1130 (w), 1109 (m), 1087 (m), 1033 (m), 947 (w), 853 (w), 821 (m), 767 (w), 679 (w), 532 (w).

Preparation of $Ni_2(BDC)_2(bimb)_2(H_2O)_2·3H_2O$ (2). A mixture containing $Ni(NO_3)_2·6H_2O$ (58.2 mg, 0.2 mmol), H_2BDC (19.3 mg, 0.1 mmol), bimb (39.2 mg, 0.1 mmol) and NaOH (8.0 mg, 0.2 mmol) in 15ml deionized water was sealed in a 25 mL Teflon lined stainless steel container and heated at 160 ºC for 3 days. Green block crystals of **2** were collected by filtration and washed with water and ethanol several times with a yield of 57% based on H_2BDC. Anal. calcd for $C_{56}H_{54}N_8O_{13}Ni_2$: C 57.76; H 4.67; N 9.62; Found: C 57.74; H 4.68; N 9.61%. IR(KBr pellet, cm^{-1}): 3471 (br), 3057 (w), 2827 (w), 1603 (s), 1585 (s), 1522 (m), 1442 (m), 1383 (s), 1288 (w), 1203(w), 1091 (m), 933 (w), 837 (m), 753 (m), 631 (w), 562 (w).

Preparation of NiZn(BTC)(titmb)Br (3). A mixture containing $Ni(NO_3)_2·6H_2O$ (29.1 mg, 0.1 mmol), $ZnBr_2$ (22.5 mg, 0.1 mmol), H_3BTC (21.0 mg, 0.1 mmol), titmb (36.0 mg, 0.1 mmol) and NaOH (12.0 mg, 0.3 mmol) in 15 ml deionized water was sealed in a 25 ml Teflon lined stainless steel container and heated at 180 ºC for 3 days. Pale green cubic crystals of **3** were collected by filtration and washed with water and

RSC Advances Accepted Manuscript

ethanol several times with a yield of 42%. Anal. calcd for $C_{30}H_{27}BrN_6O_6NiZn$: C 46.70; H 3.53; N 10.89; Found: C 46.72; H 3.56; N 10.88%. IR(KBr pellet, cm^{-1}): 3452 (br), 3092 (w), 2823 (w), 1610 (s), 1578 (s), 1520 (s), 1446 (m), 1387 (m), 1293 (m), 1250 (m), 1111 (m), 1091 (m), 1013 (m), 945 (m), 867 (w), 810 (w), 773 (m), 759 (m), 674 (w), 587 (m).

Preparation of Ni(TBDC)(titmb)(H_2O) (4).

$Ni(NO_3)_2·6H_2O$ (29.1 mg, 0.1 mmol), H_2TBDC (22.2 mg, 0.1 mmol), timb (36.0 mg, 0.1 mmol), NaOH (8 mg, 0.2 mmol) and 15 mL deionized water in a 25 mL Teflon lined stainless steel container at 160 ºC for 4 days produced green block crystals of **4** in 69% yield after washing with water and ethanol several times. Anal. Calcd for $C_{33}H_{35}N_6O_5Ni$: C 60.29; H 5.83; N 12.78; Found: C 60.28; H 5.81; N 12.77%. IR(KBr pellet, cm^{-1}): 3449 (br), 3062 (m), 1609 (s), 1571 (s), 1519 (m), 1383 (s), 1231 (w), 1093 (m), 875 (m), 822 (m), 765 (m), 716 (m), 653 (m), 569 (w), 462(w).

Preparation of Ni(TBDC)(bix)·H_2O (5).

A mixture containing $Ni(NO_3)_2·6H_2O$ (29.1 mg, 0.1mmol), H_2TBDC (22.2 mg, 0.1 mmol), bix (23.6 mg, 0.1 mmol) and $LiOH·H_2O$ (8.4 mg, 0.2 mmol) in 15 mL deionized water was sealed in a 25ml Teflon lined stainless steel container and heated at 170 ºC for 3 days. Green block crystals of **5** were collected by filtration and washed with water and ethanol several times with a yield of 48%. Anal. Calcd for $C_{33}H_{35}N_6O_5Ni$: C 60.57; H 5.39; N 12.84; Found: C 60.55; H 5.41; N 12.85%. IR(KBr pellet, cm^{-1}): 3453 (s), 3098 (w), 2823 (w), 1609 (s), 1589 (s), 1520 (m), 1442 (m), 1401 (s), 1375 (s), 1298 (w), 1126 (w), 1091 (m), 922 (m), 839 (s), 765 (m), 673

RSC Advances Accepted Manuscript

(w), 521(m).

Preparation of Ni(TBDC)(mbix)(H_2O)·H_2O (6).

The preparation of **6** was similar to that of **5** except that mbix was used instead of bix as auxiliary ligand. Green pillar crystals of **6** were collected in a 57% yield. Anal. Calcd for $C_{26}H_{30}N_4O_6Ni$: C 56.45; H 5.47; N 10.13; Found: C 56.47; H 5.48; N 10.15%. IR(KBr pellet, cm^{-1}): 3466 (m), 3159 (w), 3059 (w), 2829 (w), 1586 (s), 1522 (m), 1447 (m), 1393 (s), 1298 (w), 1103 (m), 1089 (m), 951 (m), 922 (m), 835 (w),795 (w), 744 (m), 711 (m), 659 (m), 544 (w).

Preparation of Ni(TBDC)(obix)(H_2O) (7).

Complex **7** was prepared in the same way as that for **5** but using obix instead of bix as auxiliary ligand. Green block crystals of **7** were collected in a 61% yield. Anal. Calcd for $C_{26}H_{28}N_4O_5Ni$: C 58.35; H 5.27; N 10.47; Found: C 58.33; H 5.29; N 10.44%. IR(KBr pellet, cm^{-1}): 3457 (m), 3189 (m), 2826 (w), 1605 (s), 1582 (s), 1520 (m), 1441 (m), 1378 (s), 1256(m), 1179 (m), 1091 (s), 955 (w), 874 (w), 833 (s),792 (m), 745 (s), 663 (m), 555 (w).

X-Ray crystallography

Crystallographic data collections for complexes **1 - 7** were carried out on a Bruker Smart Apex II CCD with graphite-monochromated Mo-Kα radiation (λ = 0.71073 Å) at 293(2) K using the ω-scan technique. The data were integrated by using the SAINT program,[22] which was also used for the intensity corrections for the Lorentz and polarization effects. An empirical absorption correction was applied using the SADABS program.[23] The structures were solved by direct methods using the program

RSC Advances Accepted Manuscript

SHELXS-97 and all non-hydrogen atoms were refined anisotropically on F^2 by the full-matrix least-squares technique using the SHELXL-97 crystallographic software package. The hydrogen atoms of the organic ligands were refined as rigid groups. Some of the water hydrogen atoms in complex **2** could not be positioned reliably. Other hydrogen atoms of water molecules were located from difference Fourier maps. All calculations were performed on a personal computer with the SHELXL-97 crystallographic software package.[24] The details of the crystal parameters, data collection and refinement for the complexes are summarized in Table 1, and selected bond lengths and angles with their estimated standard deviations are listed in Table S1. CCDC-804097 (**1**), 733836 (**2**), 936716 (**3**), 936717 (**4**), 936718 (**5**), 936719 (**6**) and 936720 (**7**) contain the crystallographic data for this paper.

<Table 1 here>

Results and discussion

IR spectra

For complexes **1** - **7**, the observed bands of 3400 – 3400 cm^{-1} characterize water molecules in the structures, while the bands of C - H of aromatic rings at 2830 – 2820 cm^{-1}. The IR spectra show the absence of the characteristic bands at around 1700 cm^{-1} attributed to the protonated carboxylate group indicates that the complete deprotonation of the polycarboxylic acids upon reaction with metal ion. The characteristic bands of carboxyl groups are shown in the range of 1540 - 1620 cm^{-1} for

RSC Advances Accepted Manuscript

antisymmetric stretching and 1360 - 1460 cm^{-1} for symmetric stretching. The separations (Δ) between ν_{asym} (CO_2) and ν_{sym} (CO_2) bands indicate the presence of different coordination modes. The IR spectra exhibit the characteristic peaks of imidazole groups at *ca*.1520 cm^{-1}. The bands in the region 640 -1310 cm^{-1} are attributed to the -CH- in-plane or out-of-plane bend, ring breathing, and ring deformation absorptions of benzene ring, respectively. The bands in the region 640 - 1250 cm^{-1} are attributed to the -CH- in-plane or out-of-plane bend, ring breathing, and ring deformation absorptions of benzene ring, respectively.[25]

Crystal structure of Ni(BDC)(titmb)·3H_2O (1)

Complex **1** crystallizes in the orthorhombic acentric space group *Pna*2_1, the asymmetric unit contains one Ni(II) ion, one BDC^{2-} anion, one titmb ligand and three lattice water molecule. The Ni(II) ion is six-coordinated and close to an octahedron NiN_3O_3 geometry. As illustrated in Fig. 1a, three oxygen atoms (O1, O2 and O4A) belonging to two different BDC^{2-} anions and one titmb nitrogen atom (N3B) are ligated to the Ni(II) ion in the equatorial plane, with the other two nitrogen atoms (N1C and N5) arising from the titmb ligand situated in the axial position. Each Ni(II) approximately lies in the equatorial position with a maximum deviation (0.024 Å) from the basal plane. In the structure, Ni-O and Ni–N bond distances are in the range of 2.004(3)–2.200(3) and 2.043(4)–2.069(4) Å, respectively. Each titmb ligand in turn connects three Ni(II) ions which form a triangle with edge lengths (Ni···Ni) of 9.367, 11.862 and 12.954 Å, respectively. The three imidazolyl rings are inclined to the

RSC Advances Accepted Manuscript

phenyl ring with angles of 85.98º, 86.25º and 82.17º, respectively. As shown in Fig. 1b, each Ni(II) ion connects three titmb ligands and each titmb ligand connects three Ni(II) ions, such a coordination mode makes the complex a 2D network with honeycomb structure, and a schematic drawing is shown in Fig. 1c. It is obvious that all titmb ligands in the network have *cis*, *trans*, *trans*-conformation with up- and down-orientations alternatively. BDC^{2-} anions adopt monodentate and bidentate chelate coordination modes and connect the Ni-titmb layers as pillars to generate a 3D structure (Fig. 1d). If the Ni(II) ion is considered as a five-connected node (connecting to two BDC^{2-} anions and three titmb ligands), the titmb ligand can be considered as a three-connected node (connecting to three Ni(II) ions), and the structure of **1** can be classified as a rare binodal (3,5)-connected $(6^3)(6^9.8)$ topology (Fig. 1e). In addition, the 3D structure of **1** is further stabilized by intermolecular H-bonding interactions.

<Figure 1 here>

Crystal structure of $Ni_2(BDC)_2(bimb)_2(H_2O)_2\cdot 3H_2O$ (2)

Employing the bridging bimb ligand in this system, the reaction yielded complex **2** showing a much different structure from **1**. Fig. 2a illustrates the coordination environments of the Ni(II) ions. The crystallographically independent Ni(II) ion is six-coordinated by two nitrogen atoms from two different bimb ligands, three carboxylate oxygen atoms from two BDC ligands and one coordinated water molecule to construct a distorted octahedral geometry. The Ni–O bond lengths are in the range

RSC Advances Accepted Manuscript

of 2.0273(17)–2.1369(17) Å, the Ni–N bond lengths are 2.063(2) and 2.071(2) Å and the coordination angles around Ni(II) ion are in the range of 61.61(7)º–178.79(8)º. The two carboxylate groups of the BDC ligands adopting monodentate and bidentate chelate coordination modes link two Ni(II) atoms to form a one-dimensional chain with Ni···Ni distances of 10.11 Å. These chains are further extended by bimb ligands into a 2D framework. It is interesting that the Ni(II) atoms all lie in the same plane, parallel to the *ab* plane, and are joined through two types of ligands, above the plane by one kind, and below by the other kind. The connection with the BDC^{2-} anions occurs along the *a* direction, while with the bimb ligands the joining is made along the *c* direction. So, the 2D structure formed is the 4-connected (4,4)-**sql** net (Fig. 2b). The undulated layers stack in an interweaving way along the *b* direction, to generate a 3D structure with open channels (Fig. 2c). After the removal of these free water molecules, PLATON[26] calculations show that the volume of the effective void is 5.5% of the unit-cell volumes. In addition, intramolecular O1W–H1WA···O3 (2.699(3) Å), O1W–H1WB···O2W (2.752(4) Å), O2W–H2WA···O3 (2.683(4) Å) and O2W–H2WB···O3W (2.680(6) Å) hydrogen-bonding interactions exist among the lattice water molecules and carboxylate oxygen atoms, which further stabilized the 2D structure of **2** (Fig. 2d).

<Figure 2 here>

Crystal structure of NiZn(BTC)(titmb)Br (3)

RSC Advances Accepted Manuscript

X-ray single crystal diffraction analysis reveals that the asymmetric unit of **3** consists of one nickel ion and one unique zinc ion (the Ni : Zn ratio of 1 : 1 based on ICP analysis) bridged by three carboxylate groups, one crystallographically independent titmb ligand, one individual BTC^{3-} anion and one coordinated bromide ion. As shown in Fig. 3a, each Zn(II) ion is tetrahedral coordinated by three oxygen atoms (O2, O2A and O2B) from three different BTC^{3-} anions and one terminal bromide ion (Br1). Each Ni(II) ion is surrounded by three nitrogen atoms (N1, N1C and N1D) from three distinct titmb ligands and three oxygen atoms (O1, O1C and O1D) from three different BTC^{3-} anions to furnish a distorted octahedral geometry. One Zn(II) ion and one Ni(II) ion are connected by three carboxylate groups in a bidentate-bridging fashion to form a binuclear $ZnNi(CO_2)_3Br$ unit, as exhibited in Fig. 3b. Each BTC^{3-} anion connect with three Zn ions and three Ni ions from three different binuclear units and each titmb ligand bridges three Ni ions from three individual binuclear units, thus each binuclear unit is linked by six organic ligands (three titmb ligands and three BTC^{3-} anions) to generate a (3,6)-connected network. The overall 3D network is so intricate that it is described in terms of two subnets. For the first subnet, the titmb ligands are omitted, the binuclear units can be considered 3-connected nodes. Each binuclear unit is bridged to three different BTC^{3-} anions. Thus the whole subnet structure can be extended to a slightly distorted (10,3)-a net with left-handedness of helices in the direction of *c* axis as shown in Fig. 3c. The extended Schläfli symbol of this net is $10_5.10_5.10_5$. From another point of view, the BTC^{3-} anions are ignored for the second subnet. Interestingly, a heavily distorted (10,3)-a net with right-handedness

RSC Advances Accepted Manuscript

of helices is obtained as displayed in Fig. 3d. It is obvious that all titmb ligands in the network have *cis, cis, cis*-conformation.

To describe the overall topology of complex **3**, we add the titmb ligand to the first subnet or add the BTC^{3-} ligand two the second subnet. Thus we get an unprecedented $(6^3)_2(6^{12}.8^3)$ net calculated by the TOPOS program[27] (Fig. 3e). To the best of our knowledge, the network represents a novel (3,6)-connected topology which is different from the rutile and rutile-related topology[28] by self-penetration of two sets of (10,3)-a nets.

<Figure 3 here>

Crystal structure of Ni(TBDC)(titmb)(H_2O) (4)

The polymeric structure of **4** was confirmed by X-ray single crystal structure analysis. The complex crystallizes in the orthorhombic space group $P2_12_12_1$ and Fig. 4a shows the asymmetric unit of **4** with atom numbering scheme. Each Ni(II) atom is coordinated by three imidazole nitrogen atoms derived from three different timb ligands and three oxygen atoms from two different $TBDC^{2-}$ ligands and one water molecule. The coordination geometry of the Ni(II) center is a slightly distorted octahedron with coordination angles ranging from 85.22(10)º to 175.26(11)º and the Ni–O/N bond lengths varying from 2.040(2) to 2.144(3) Å (Table S1). Each timb ligand in turn connects three Ni(II) atoms which form a triangle with edge lengths (Ni···Ni) of 8.01, 10.58 and 13.29 Å, respectively. The three imidazolyl rings are

RSC Advances Accepted Manuscript

inclined to the phenyl ring with angles of 73.24º, 69.23º and 59.21º, respectively. As shown in Fig. 4b, such a coordination mode makes the compound a 2D network with a honeycomb structure, and a schematic drawing is shown in Fig. 4c. It is obvious that all timb ligands in the network have *cis*, *trans*, *trans*-conformation with up- and down-orientations alternatively. $TBDC^{2-}$ ligands adopt monodentate and chelate coordination modes and connect two Ni(II) atoms of the Ni-timb layers to generate a 2D structure (Fig. 4d). If the Ni(II) atom is considered as a five-connected node (connecting to two TBDC anions and three timb ligands), the timb ligand can be considered as a three-connected node (connecting to three Ni atoms), and the structure of **4** can be classified as a rare (3,5)-connected 2D framework with $(3.5^2)(3^2.5^3.6^4.7)$ topology (Fig. 4e). In addition, the 3D supramolecular structure of **4** is further extended by C-H···π interactions.

<Figure 4 here>

Crystal structure of Ni(TBDC)(bix)·H_2O (5)

Single crystal X-ray diffraction analysis reveals that complex **5** crystallizes in the triclinic space group *P*-1 and the asymmetric unit of **5** is constructed from one Ni(II) ion, one fully deprotonated $TBDC^{2-}$ ligand, one and a half bix ligands and one lattice water molecule (Fig. 5a). The Ni(II) ion is coordination by three carboxylic oxygen atoms from two different $TBDC^{2-}$ ligands and three imidazolyl nitrogen atoms from three bix ligands in a slightly distorted $[NiO_3N_3]$ octahedral geometry. The three

RSC Advances Accepted Manuscript

coordinated carboxyl oxygen atoms together with two imidazolyl nitrogen atoms define the equatorial positions, while the axial positions are occupied by two imidazolyl nitrogen atoms. The Ni–O bond distances are in the range of 2.016(2)–2.234(2) Å while the Ni–N bond distances are in the range of 2.048(3)–2.092(3) Å, which are all in good agreement with those reported for other nickel–oxygen and nickel–nitrogen donor compounds.[29] The $TBDC^{2-}$ ligand exhibist η^2-η^1 coordination mode with one of the two carboxylate groups adopts chelating coordination mode while the other one holds a monodentate bridging mode. The Ni(II) atoms are first linked by the $TBDC^{2-}$ linkers to form 1D chain as shown in Fig. 5b. Meanwhile, the Ni(II) centers are also bridged by bix ligands to form 2D layers with (6, 3) topology as shown in Fig. 5c. Then these chains and layers are cross-connected with each other to form five-connected 3D framework with $(4^6.6^4)$-**bnn** hexagonal BN topology in which the Ni(II) ions act as unimodal center (Fig. 5d). Further investigation into the topology of complex **5** reveals that there are two identical independent 3D networks that interpenetrate with each other (Fig. 5e). The two 3D subunits are related to each other by one translation. In a word, the structure of **5** exhibits a 3D coordination network with two-fold interpenetration of subunits with $(4^6.6^4)$-**bnn** hexagonal BN topology.

<Figure 5 here>

Crystal structure of Ni(TBDC)(mbix)(H_2O)·H_2O (6)

In order to investigate the influence of auxiliary ligand on the structure of the

RSC Advances Accepted Manuscript

complexes, reactions of $Ni(NO_3)_2 \cdot 6H_2O$ with H_2TBDC in the presence of mbix were carried out and complex **6** was obtained. As displayed in Fig. 6a, the asymmetric unit of **6** contains crystallographically unique Ni(II) ion, one TBDC anion, one mbix ligand, one coordinated water molecule and one lattice water molecule. The Ni(II) center is six-coordinated by three carboxylate oxygen atoms from two individual TBDC anions, two nitrogen atom from two different mbix ligands and one water molecule, displaying a distorted octahedral coordination geometry. Each TBDC anion links two Ni(II) ions with its two carboxylate groups adopting monodentate and bidentate chelating modes. The mbix ligands connected adjacent Ni(II) ions to afford a 1D zigzag chain. If mbix ligands are neglected, Ni(II) ions are bridged by TBDC anions to form a 1D wavelike chain. The two types of chains are linked to generate 2D layers through sharing the central Ni(II) ions. Notably, the network has large rhombic windows with approximate dimensions of 9.00 × 20.60 $Å^2$ built up by four Ni(II) ions, two mbix ligands, and two TBDC anions within the 2D motif (Fig. 6b). For convenience, if Ni(II) ions are viewed as uninodal 4-connected nodes, and TBDC anions and mbix ligands are viewed as linkers, the layer can be described as a 4-connected **sql** topology with the point Symbol of $4^4.6^2$ (Fig. 6c). In addition, there exist π-π stacking interactions associated with phenyl rings of TBDC anions and phenyl rings of mbix ligands (face-to-face distance of 3.85 Å and centroid-to-centroid distance of 3.63 Å) in the adjacent layers. These π-π interactions among layers led the2D sheets to a 3D supramolecular architecture (Fig. 6d).

RSC Advances Accepted Manuscript

<Figure 6 here>

Crystal structure of Ni(TBDC)(obix)(H_2O) (7)

The crystallographic analysis reveals that **7** is a one-dimensional tubular structure. As shown in Fig. 7a, the asymmetric unit contains one Ni(II) ion, one $TBDC^{2-}$ anion, one obix ligand and one coordinated water molecule. Each Ni(II) ion is six-coordinated by four oxygen atoms from two different $TBDC^{2-}$ anion and one water molecule, and two nitrogen atoms from two obix ligands to form a distorted octahedral geometry and its basal plane is occupied by four oxygen atoms, while the apical position is occupied by two nitrogen atom. The Ni-O bond lengths are in the range of 2.0227(18) - 2.1634(18) Å, the Co-N bond lengths are 2.071(2) –2.086(2) Å and the coordination angles around Co ion are in the range of 61.24(7) - 176.82(9)°. Two Ni(II) ions are linked by a couple of obix ligands to form 24-membered $\{Ni_2(obix)_2\}$ ring and the distance of neighboring Ni(II) ions is about 5.284 Å as presented in Fig. 7b. The obix ligand adopts a *cis*-conformation with the dihedral angle between the two imidazole rings of 58.57º. Two carboxylate groups of $TBDC^{2-}$ ligand adopt monodentate and bidentate chelating coordination mode and link to the neighboring $\{Ni_2(obix)_2\}$ rings, giving a one-dimensional tubular structure. The separation of neighboring Ni(II) ions is about 10.24 Å as illustrated in Fig. 7c. The packing structure of **7** shows a three-dimensional supramolecular network derived from chains formed *via* intermolecular C-H···O hydrogen bonds and weak π-π stacking interactions (the centroid-to-centroid distance of 4.125 Å between the two adjacent benzene rings of TBDC ligands and benzene

RSC Advances Accepted Manuscript

rings of obix ligands, and the dihedral angle is 5.302(5)°).

<Figure 7 here>

In this work, we selected imidazole-containing ligands and three different aromatic dicarboxylates to construct seven target metal complexes, aiming at examining the effect of substituent groups, the number of the carboxylic groups as well as the auxiliary ligands on the assembly and structures of the resulting products. Compared with related structures in the literature, $Co_3(BIPA)_3(titmb)_2]\cdot 0.73H_2O$ (**8**) and Ni(mbix)(BDC)(H_2O) (**9**) (H_2BIPA = 5-bromoisophthalic acid).[15l,20b] In complexes **1**, **4** and **8**, there exist the same metal coordination geometries and auxiliary ligand, similar aromatic dicarboxylates and entirely different topological structures: a 3D (3,5)-connected binodal $(6^3)(6^9.8)$ topology framework for **1**, a 2D (3,5)-connected $(3.5^2)(3^2.5^3.6^4.7)$ topology framework for **4** and a 3D (3,4)-connected coordination framework with the topology of $(4.6.8)(4.62.8^3)(6.8^5)(6^2.8^3.10)(8^3)$ for **8**, which are attributed to the effect of 5-substituent groups. Whereas complex **6** has a 2D lamella structure with (4,4) topology, complex **9** exhibits a rare (3,5)-connected 3D network with $(4^2.6^5.8^3)(4^2.6)$ topology. The presence of the noncoordinating groups in dicarboxylate ligands changes their electronic and steric properties, which can generate complexes different from those of the common dicarboxylate ligands. The Ni(II) ions are bridged by 1,3-benzenedicarboxylates to form 1D chains in **1** and the Ni(II) ions are linked through 1,3,5-benzenetricarboxylates to generate 3D network in

RSC Advances Accepted Manuscript

3, and the results in the changes of the number of the carboxylic group, finally, causes the difference between the frameworks of **1** and **3**. In this study, complexes **4** - **7** display a diversity of 1D, 2D and 3D frameworks, and the connectivities of the four complexes are strongly related to the imidazole-containing ligands. As described above, the imidazole-containing ligands serve as bridging ligands with nitrogen atoms of the imidazole units coordinating to the metal atoms. In **4**, Ni(II) ions are linked by titmb ligands to form a 2D network with a honeycomb structure; in **5**, the Ni(II) centers are also bridged by bix ligands to form 2D layers with (6, 3) topology. In **6**, Ni(II) centers are bridged by mbix ligands to form zigzag chains and helices simultaneously; in **7**, Ni(II) ions are linked by obix ligands to form [Ni(obix)$_2$Ni] dimers.

Thermogravimetric analyses

To estimate the stability of the coordination architectures of complexes **1** - **7**, thermogravimetric analyses (TGA) were carried out. The experiments were performed on samples consisting of numerous single crystals of **1**-**7** under a N_2 atmosphere with a heating rate of 10 °C min^{-1} (Fig. 8). The TGA curves show that first a weight loss occurs in the range of 40-180 °C (obsd 8.20%, calcd 8.47%) for **1**, which corresponds to the free water molecules, and indicating that there exist strong hydrogen-bonding interactions among the water molecules. The second weight loss was observed from 290 to 600 °C (obsd 12.4%, calcd 13.0%), showing the departure of organic ligands. Finally, the remaining weight corresponds to the oxidized metal. Complex **2** loses the two lattice water molecules and three coordinated water molecules in the range of 40

RSC Advances Accepted Manuscript

– 198 °C (obsd 7.4% and calcd 7.7%). The removal of water at a high temperature is attributed to the strong hydrogen-bonding interactions. Further weight loss occurs from 267 to 570°C (obsd 70.0% and calcd 78.0%), indicating organic ligands loss and complex decomposition. The final residual weight corresponds to that of Ni_2O_3 (obsd 14.5%, calcd 14.2%). The TGA curve of **3** reveals that no obvious weight loss was observed until the temperature rose to 290°C. The anhydrous compound decomposes from 290 to 600°C (obsd 75.8 %, calcd 78.3%), indicating the release of organic components. For **4**, the weight loss before 160 °C corresponds to the release of coordinated water molecules (obsd 2.89%, calcd 2.74%), and the weight loss between 230 and 620 °C is attributable to the departure of organic components (obsd 78.2%, calcd 84.7%). The residual is oxidized metal (obsd 11.3 %, calcd 12.6 %). The TG curve for **5** reveals that the first weight loss of lattice water molecules is observed from room temperature to 165 °C (obsd 2.9%, calcd 2.8 %), which shows that there exist strong hydrogen-bonding interactions between the water molecules at high temperature. The second weight loss occurs in the range of 250–630 °C (obsd 78.5%, calcd 84.6 %), revealing that the compound decomposes. Finally, the residual is Ni_2O_3 (obsd 13.2%, calcd 12.7%). The first weight loss for complex **6** from 45 to 177 °C corresponds to the elimination of one lattice water and one coordinated water (obsd 6.4% and calcd 6.5%). The second weight loss occurs between 210-620 °C (obsd 76.2%, calcd 78.5%), which may be assigned to the removal of organic ligands. After that, the weight loss is slow, and finally yields the residual oxidised metal at 620 °C (obsd 16.2% and calcd 15.0%). The TGA curve for **7** shows that a weight loss of 3.6%

RSC Advances Accepted Manuscript

occurs in range of 80–172 °C, which may be attributed to the removal of one coordinated water molecule (obsd 3.1% and calcd 3.4%). Further, a weight loss occurs in the range of 295–620 °C (obsd 76.9%, calcd 82.0%). There is no mass loss from 190 to 290 °C, indicating a relatively higher thermal stability.

SHG response

As mentioned in the introduction, CPs show interesting non-linear optical properties (NLO) and second harmonic generation (SHG) responses. SHG is completely dependent on crystal symmetry and SHG materials have been extensively applied to high technique fields such as laser devices and optical communications. Generally, an SHG-active material must require the absence of a symmetric center. Lin, Xiong, Chen and coworkers illustrated that CPs with noncentrosymmetric structures can be rationally designed and prepared by making use of metal ions with specific geometries and high directional coordination bonds.[30] Thus, rationally designing and synthesizing CPs with SHG responses has enabled us to understand the relationships between structures and properties. Considering that complexes **1**, **3** and **4** crystallize in the acentric space group ($Pna2_1$, $P2_13$ or $P2_12_12_1$), their nonlinear optical properties were studied.[31] The strength of the second harmonic generation (SHG) efficiency of complexes **1**, **3** and **4** was tested by measuring the microcrystalline powder samples with 61–90 μm in diameters. Preliminary examinations indicate that complexes **1**, **3** and **4** are SHG-active and the SHG efficiency is approximately 0.8, 0.6, and 0.7 times that of urea, respectively, which indicates that complexes **1**, **3** and **4** have potential

RSC Advances Accepted Manuscript

application in optical material. The modest powder SHG response of complexes **1**, **3** and **4** may be attributed to a comparatively short donor–acceptor system, which is essential for second-order optical nonlinearity.

Recently, a prevalent research has focused on developing ferroelectric materials based on coordination polymers (CPs) and have reported some such materials.[32] However, the reported ferroelectric materials are mostly built upon chiral organic tectons, whereas the proper use of achiral ligands by spontaneous are scarce.[33] Herein, we describe the preliminary investigation of the possible ferroelectric property of complex **1**. Complex **1** crystallizes in the acentric space group $Pna2_1$, which belongs to the polar point group C_{2v}, which falls in one of the 10 polar point groups (*C*1, *Cs*, *C*2, *C*2*v*, *C*4, *C*4*v*, *C*3, *C*3*v*, *C*6, *C*6*v*) required for ferroelectric materials. Therefore, the ferroelectric behavior of **1** was examined. Fig. 9 clearly shows that there is an electric hysteresis loop that is a typical ferroelectric feature with a remanent polarization (*Pr*) of *ca*. 0.049 μC cm^{-2} and coercive field (*Ec*) of *ca*. 850 V cm^{-1}. The saturation spontaneous polarization (*Ps*) of **1** is *ca*. 0.21 μC cm^{-2}, which is slightly lower than that of Rochelle salt ($NaKC_4H_4O_6{\cdot}4H_2O$, *Ps* = 0.25 μC cm^{-2}).[34] The value of *Ps* is comparable to that of some CPs reported in the literature.[35] Furthermore, we also studied the behavior of permittivity (ε) = $\varepsilon_1(\omega) - i\varepsilon_2(\omega)$, where $\varepsilon_1(\omega)$ and $i\varepsilon_2(\omega)$ are the real (dielectric constant) and imaginary (dielectric loss) parts, respectively. The results reveal that the frequency dependence of the dielectric constant ε_1 at room temperature (20 ºC) indicates that ε_1 rapidly decreases with the increase of frequency, while dielectric loss remains unchanged.

RSC Advances Accepted Manuscript

<Figure 8 here>

Conclusions

In this work, we have successfully fabricated seven novel coordination polymers under hydrothermal condition. Complex **1** shows a three-dimensional (3D) (3,5)-connected network with the topology of $(6^3)(6^9.8)$. Complexes **2** and **6** have similar two-dimensional (2D) lamella structure with (4,4) topology. Complex **3** exhibits an interesting 3D (3,6)-connected framework by self-penetration of two sets of (10,3)-a nets. Complex **4** presents a unusual 2D (3,5)-connected framework with the topology of $(3.5^2)(3^2.5^3.6^4.7)$. Complex **5** features a 3D two-fold interpenetrating framework with $(4^6.6^4)$-**bnn** hexagonal BN topology, whereas Complex **7** possesses an interesting one-dimensional (1D) independent single-wall metal-organic nanotube. The various dimensions and structural features of the seven complexes may be attributed to the different species of functional groups, the number and position of the carboxylic groups in the carboxylates as well as the auxiliary ligands. Additionally, the ferroelectric and NLO properties of the imidazole and carboxylate system have been investigated, and open up a new avenue to NLO and ferroelectric materials through CPs.

Acknowledgements

This work was supported by the National Natural Science Foundation of China (Nos.

RSC Advances Accepted Manuscript

21271116, 21171097), the Key Project of Chinese Ministry of Education (No. 210102) and the Qing Lan Project of Jiangsu Provincial Department of Education.

References

1 (*a*) Y. Kang, F. Wang, J. Zhang and X. Bu, *J. Am. Chem. Soc.*, 2012, **134**, 17881; (*b*) R. B. Getman, Y. S. Bae, C. E. Wilmer and R. Q. Snurr, *Chem. Rev*., 2012, **112**, 703; (*c*) D. S. Li, Y. P. Wu, J. Zhao, J. Zhang and J. Y. Lu, *Coord. Chem. Rev.*, 2014, **261**, 1; (*d*) L. Q. Ma, C. Abney and W. B. Lin, *Chem. Soc. Rev.*, 2009, **38**, 1248; (*e*) W. W. Zhou, J. T. Chen, G. Xu, M. S. Wang, J. P. Zou, X. F. Long, G. J. Wang, G. C. Guo and J. S. Huang, *Chem. Commun.*, 2008, 2762; (*f*) T. Hang, W. Zhang, H. Y. Ye and R. G. Xiong, *Chem. Soc. Rev.*, 2011, **40**, 3577; (*g*) Z. G. Guo, R. Cao, X. Wang, H. F. Li, W. B. Yuan, G. J. Wang, H. H. Wu and J. Li, *J. Am. Chem. Soc.*, 2009, **131**, 6894; (*h*) W. W. Xiong, E. U. Athresh, Y. T. Ng, J. Ding, T. Wu and Q. Zhang, *J. Am. Chem. Soc.*, 2013, **135**, 1256.

2 (*a*) W. Xuan, C. Zhu, Y. Liu and Y. Cui, *Chem. Soc. Rev.*, 2012, **41**, 1677; (*b*) S. R. Batten, N. R. Champness, X. M. Chen, J. Garcia-Martinez, S. Kitagawa, L. Ohrstrom, M. O'Keeffe, M. P. Suh and J. Reedijk, *Pure Appl. Chem.*, 2013, **85**, 1715; (*c*) X. Xi, Y. Liu and Y. Cui, *Inorg. Chem.*, 2014, **53**, 2352; (*d*) S. M. F. Vilela, J. A. Fernandes, D. Ananias, L. D. Carlos, J. Rocha, J. P. C. Tome and F. A. A. Paz, *CrsytEngComm*, 2014, **16**, 344; (*e*) S. Freslon, Y. Luo, G. Calvez, C. Daiguebonne, O. Guillou, K. Bernot, V. Michel and X. Fan, *Inorg. Chem.*, 2014, **53**, 1217; (*f*) C. Zhang, M. Zhang, L. Qin and H. Zheng, *Cryst. Growth Des.*,

RSC Advances Accepted Manuscript

2014, **14**, 491; (*g*) Y. X. Tan, Y. P. He and J. Zhang, *Chem. Mater.*, 2012, **24**, 4711; (*h*) Y. Zhao, D. S. Deng, L. F. Ma, B. M. Ji and L. Y. Wang, *Chem. Commun.*, 2013, **49**, 10299.

3 (a) M. H. Zeng, Y. X. Tan, Y. P. He, Z. Yin, Q. Chen and M. Kurmoo, *Inorg. Chem.*, 2013, **52**, 2353; (*b*) T. R. Cook, Y. R. Zheng and P. J. Stang, *Chem. Rev.*, 2013, **113**, 734; (*c*) Q. Zhai, Q. Lin, T. Wu, L. Wang, S. Zheng, X. Bu and P. Feng, *Chem. Mater.*, 2012, **24**, 2624; (*d*) G. Q. Kong, S. Ou, C. Zou and C. D. Wu, *J. Am. Chem. Soc.*, 2012, **134**, 19851; (*e*) M. I. Bodnarchuk, R. Erni, F. Krumeich and M. V. Kovalenko, *Nano Lett.*, 2013, **13**, 1699; (*f*) Y. Liu, K. Mo and Y. Cui, Inorg. Chem., 2013, 52, 10286; (*g*) V. Bon, I. Senkovska, D. Wallacher, D. M. Többens, I. Zizak, R. Feyerherm, U. Mueller and S. Kaskel, *Inorg. Chem.*, 2014, **53**, 1513; (*h*) B. Bhattacharya, R. Haldar, R. Dey, T. K. Maji and D. Ghoshal, *Dalton Trans.*, 2014, **43**, 2272.

4 (*a*) P. Wang, R. Q. Fan, X. R. Liu, L. Y. Wang, Y. L. Yang, W. W. Cao, B. Yang, W. Hasi, Q. Su and Y. Mu, *CrystEngComm*, 2013, **15**, 1931; (*b*) Y. P. He, Y. X. Tan and J. Zhang, *Inorg. Chem.*, 2013, **52**, 12758; (*c*) J. Li, J. Zhang, M. G. Humphrey and C. Zhang, *Eur. J. Inorg. Chem.*, 2013, 328; (*d*) B. Moulton and M. J. Zaworotko, *Chem. Rev.*, 2011, **101**, 1629; (*e*) G. P. Zhou, Y. L. Yang, R. Q. Fan, W. Cao and B. Yang, *CrystEngComm*, 2012, **14**, 193; (*f*) P. Wang, R. Q. Fan, Y. L. Yang, X. R. Liu, W. W. Cao and B. Yang, *J. Solid State Chem*., 2012, **196**, 441; (*g*) R. Q. Fan, L. Y. Wang, P. Wang, H. Chen, C. F. Sun, Y. L. Yang and Q. Su, *J. Solid State Chem.*, 2012, **196**, 332.

RSC Advances Accepted Manuscript

5 (*a*) Y. Liang, Z. M. Zhang, Z. J. Liu, Y. Zhang, J. Zhang and E. B. Wang, *CrystEngComm*, 2014, **16**, 1187; (*b*) A. Masello, K. A. Abboud, W. Wernsdorfer and G. Christou, *Inorg. Chem*., 2013, **52**, 10414; (*c*) Y. Q. Lan, S. L. Li, X. L. Wang, K. Z. Shao, Z. M. Su and E. B. Wang, *Inorg. Chem*., 2008, **47**, 529; (*d*) Y. Z. Zheng, Z. Zheng and X. M. Chen, *Coord. Chem. Rev*., 2014, **258**, 1; (*e*) S. Biswas, H. S. Jena, S. Goswami, S. Sanda and S. Konar, *Cryst. Growth Des*., 2014, **14**, 1287; (*f*) Z. Chen, L. Liu, Y. Wang, H. H. Zou, Z. Zhang and F. Liang, *Dalton Trans*., 2014, **43**, 8154; (*g*) A. Kondo, H. Kajiro, H. Noguchi, L. Carlucci, D. M. Proserpio, G. Ciani, K. Kato, M. Takata, H. Seki, M. Sakamoto, Y. Hattori, F. Okino, K. Maeda, T. Ohba, K. Kaneko and H. Kanoh, *J. Am. Chem. Soc.*, 2011, **133**, 10512.

6 (*a*) M. D. Zhang, H. G. Zheng, Z. Z. Lu and X. Q. Yao, *CrystEngComm*, 2013, **15**, 9265; (*b*) C. Wang, T. Zhang and W. Lin, *Chem. Rev*., 2012, **112**, 1084; (*c*) Z. Jin, H. He, H. Zhao, T. Borjigin, F. Sun, D. Zhang and G. Zhu, *Dalton Trans*., 2013, **42**, 13335; (*d*) Z. Zhang, L. Zhang, L. Wojtas, M. Eddaoudi and M. J. Zaworotko, *J. Am. Chem. Soc.*, 2012, **134**, 928; (e) Y. Cui, Y. Yue, G. Qian and B. Chen, *Chem. Rev.*, 2012, **112**, 1126; (*f*) R. Chen, J. Yao, Q. Gu, S. Smeets, C. Baerlocher, H. Gu, D. Zhu, W. Morris, O. M. Yaghi and H. Wang, *Chem. Commun.*, 2013, **49**, 9500; (*g*) L. Wen, L. Zhou, B. Zhang, X. Meng, H. Qu and D. Li, *J. Mater. Chem.*, 2012, **22**, 22603.

7 (*a*) S. D. Han, W. C. Song, J. P. Zhao, Q. Yang, S. J. Liu, Y. Li and X. H. Bu, *Chem. Commun*., 2013, **49**, 871; (*b*) Y. Y. Xu, X. X. Wu, Y. Y. Wang, X. M. Su, S.

RSC Advances Accepted Manuscript

X. Liu, Z. Z. Zhu, B. Ding, Y. Wang, J. Z. Huo and G.X. Du, *RSC Adv*., 2014, **4**, 25172; (*c*) Y. L. Hou, G. Xiong, P. F. Shi, R. R. Cheng, J. Z. Cui and B. Zhao, *Chem. Commun*., 2013, **49**, 6066; (*d*) G. S. Yang, Z. L. Lang, H. Y. Zang, Y. Q. Lan, W. W. He, X. L. Zhao, L. K. Yan, X. L. Wang and Z. M. Su, *Chem. Commun*., 2013, **49**, 1088; (*e*) J. P. Zou, Q. Peng, Z. Wen, G. S. Zeng, Q. J. Xing and G. C. Guo, *Cryst. Growth Des*., 2010, **10**, 2613; (*f*) X. Zou, H. Ren and G. Zhu, *Chem. Commun*., 2013, **49**, 3925.

8 (*a*) W. Kaneko, S. Kitagawa and M. Ohba, *J. Am. Chem. Soc.*, 2007, **129**, 248; (*b*) Z. G. Guo, R. Cao, X. Wang, H. F. Li, W. B. Yuan, G. J. Wang, H. H. Wu and J. Li, *J. Am. Chem. Soc.*, 2009, **131**, 6894; (*c*) T. Hang, W. Zhang, H. Y. Ye and R. G. Xiong, *Chem. Soc. Rev*., 2011, **40**, 3577; (*d*) W. W. Zhou, J. T. Chen, G. Xu, M. S. Wang, J. P. Zou, X. F. Long, G. J. Wang, G. C. Guo and J. S. Huang, *Chem. Commun.*, 2008, 2762.

9 (*a*) X. Q. Yao, D. P. Cao, J. S. Hu, Y. Z. Li, Z. J. Guo and H. G. Zheng, *Cryst. Growth Des*., 2011, **11**, 231; (*b*) J. Y. Lee, C. Y. Chen, H. M. Lee, E. Passaglia, F. Vizza and W. Oberhauser, *Cryst. Growth Des*., 2011, **11**, 1230; (*c*) J. P. Zhao, B. W. Hu, Q. Yang, T. L. Hu and X. H. Bu, *Inorg. Chem*., 2009, **48**, 7111; (*d*) A. Datta, K. Das, J. Y. Lee, Y. M. Jhou, C. S. Hsiao, J. H. Huang and H. M. Lee, *CrystEngComm*, 2011, **13**, 2824; (*e*) S. C. Sahoo, T. Kundu and R. Banerjee, *J. Am. Chem. Soc*., 2011, **133**, 17950.

10 (*a*) Y. Chen, L. Li, Z. Chen, Y. Liu, H. Hu, W. Chen, W. Liu, Y. Li, T. Lei, Y. Cao, Z. Kang, M. Lin and W. Li, *Inorg. Chem*., 2012, **51**, 9705; (*b*) X. G. Guo, W. B.

RSC Advances Accepted Manuscript

Yang, X. Y. Wu, K. Zhang, L. Lin, R. M. Yu and C. Z. Lu, *CrystEngComm*, 2013, **15**, 3654; (*c*) C. X. Chen, Q. K. Liu, J. P. Ma and Y. B. Dong, *J. Mater. Chem.*, 2012, **22**, 9027; (*d*) Z. J. Lin and M. L. Tong, *Coord. Chem. Rev.*, 2011, **255**, 421; (*e*) T. Liu, S. Wang, J. Lu, J. Dou, M. Niu, D. Li and J. Bai, *CrystEngComm*, 2013, **15**, 5476; (*f*) X. Bao, P. H. Guo, W. Liu, J. Tucek, W. X. Zhang, J. D. Leng, X. M. Chen, I. Gural'skiy, L. Salmon, A. Bousseksou and M. L. Tong, *Chem. Sci.*, 2012, **3**, 1629; (*g*) X. L. Zhao, D. Sun, S. Yuan, S. Y. Feng, R. Cao, D. Q. Yuan, S. N. Wang, J. M. Dou and D. F. Sun, *Inorg. Chem.*, 2012, **51**, 10350; (*h*) S. N. Wang, Y. Q. Peng, X. L. Wei, Q. F. Zhang, D. Q. Wang, J. M. Dou, D. C. Li and J. F. Bai, *CrystEngComm*, 2011, **13**, 5313; (*i*) L. M. Fan, X. T. Zhang, D. C. Li, D. Sun, W. Zhang and J. M. Dou, *CrystEngComm*, 2013, **15**, 349.

11 (*a*) X. Zhang, L. Hou, B. Liu, L. Cui, Y. Y. Wang and B. Wu, *Cryst. Growth Des.*, 2013, **13**, 3177; (*b*) Z. Q. Shi, Y. Z. Li, Z. J. Guo and H. G. Zheng, *Cryst. Growth Des.*, 2013, **13**, 3078; (*c*) D. Sun, Z. H. Yan, V. A. Blatov, L. Wang and D. F. Sun, *Cryst. Growth Des.*, 2013, **13**, 1277; (*d*) B. L. Chen, N. W. Ockwig, F. R. Fronczek, D. S. Contreras and O. M. Yaghi, *Inorg. Chem.*, 2005, **44**, 181; (*e*) S. Yang, X. Lin, A. J. Blake, K. M. Thomas, P. Hubberstey, N. R. Champness and M. Schröder, *Chem. Commun.*, 2008, 6108; (*f*) H. S. Choi and M. P. Suh, *Angew. Chem., Int. Ed.*, 2009, **48**, 6865; (*g*) B. L. Chen, N. W. Ockwig, A. R. Millward, D. S. Contreras and O. M. Yaghi, *Angew. Chem., Int. Ed.*, 2005, **44**, 4745; (*h*) J. L. Liu, W. Q. Lin, Y. C. Chen, J. D. Leng, F. S. Guo and M. L. Tong, *Inorg. Chem.*, 2013, **52**, 457; (*i*) P. H. Guo, J. L. Liu, Z. M. Zhang, L. Ungur, L. F. Chibotaru, J.

RSC Advances Accepted Manuscript

644 D. Leng, F. S. Guo and M. L. Tong, I*norg. Chem*., 2012, **51**, 1233; (*j*) A. H.
645 Shelton, I. V. Sazanovich, J. A. Weinstein and M. D. Ward, *Chem. Commun*.,
646 2012, **48**, 2749.
647 12 (*a*) B. Li, L. Q. Chen, R. J. Wei, J. Tao, R. B. Huang, L. S. Zheng and Z. P. Zheng,
648 *Inorg. Chem.*, 2011, **50**, 424; (*b*) W. G. Lu, D. C. Zhong, L. Jiang and T. B. Lu,
649 *Cryst. Growth Des.*, 2012, **12**, 3675; (*c*) F. L. Yang, J. Tao, R. B. Huang and L. S.
650 Zheng, *Inorg. Chem*., 2011, **50**, 911; (*d*) X. J. Zhang, M. A. Ballem, M. Ahren, A.
651 Suska, P. Bergman and K. Uvdal, *J. Am. Chem. Soc.*, 2010, **132**, 10391; (*e*) J. Ma,
652 F. L. Jiang, L. Chen, M. Y. Wu, S. Q. Zhang, K. C. Xiong, D. Han and M. C.
653 Hong, *CrystEngComm*, 2012, **14**, 4181; (*f*) L. Cheng, L. M. Zhang, S. H. Gou, Q.
654 N. Cao, J. Q. Wang and L. Fang, *CrystEngComm*, 2012, **14**, 4437; (*g*) P. Cui, L.
655 Ren, Z. Chen, H. Hu, B. Zhao, W. Shi and P. Cheng, *Inorg. Chem*., 2012, **51**,
656 2303; (*h*) W. X. Chen, H. R. Xu, G. L. Zhuang, L. S. Long, R. B. Huang and L. S.
657 Zheng, *Chem. Commun*., 2011, **47**, 11933; (*i*) G. X. Liu, H. Xu, H. Zhou, S.
658 Nishihara and X. M. Ren, *CrystEngComm*, 2012, **14**, 1856; (*j*) Q. H. Chen, F. L.
659 Jiang, L. Chen, M. Yang and M. C. Hong, *Chem. -Eur. J.*, 2012, **18**, 9117; (*k*) B.
660 Li, X. M. Dai, X. G. Meng, T. L. Zhang, C. M. Liu and K. C. Yu, *Dalton Trans*.,
661 2013, **42**, 2588; (*l*) F. Yu and B. Li, *CrystEngComm*, 2011, **13**, 7025; (*m*) Y. Y. Yin,
662 X. Y. Chen, X. C. Cao, W. Shi and P. Cheng, *Chem. Commun*., 2012, **48**, 705.
663 13 (*a*) X. Zhang, Z. H. Yi, L. Y. Zhao, Q. Chen, X. L. Wang, J. Q. Xu, W. J. Xia and
664 C. Yang, *CrystEngComm*, 2010, **12**, 595; (*b*) L. S. Long, *CrystEngComm*, 2010,
665 **12**, 1354; (*c*) M. Chen, S. S. Chen, T. A. Okamura, Z. Su, M. S. Chen, Y. Zhao, W.

RSC Advances Accepted Manuscript

Y. Sun and N. Ueyama, *Cryst. Growth Des*., 2011, **11**, 1901; (*d*) G. C. Ou, X. L. Feng and T. B. Lu, *Cryst. Growth Des*., 2011, **11**, 851; (*e*) H. X. Yang, S. Y. Gao, J. Lu, B. Xu, J. X. Lin and R. Cao, *Inorg. Chem*., 2010, **49**, 736; (*f*) H. Y. Liu, J. Yang, Y. Y. Liu and J. F. Ma, *Dalton Trans*., 2012, **41**, 9922; (*g*) D. Sun, Z. H. Wei, C. F. Yang, D. F. Wang, N. Zhang, R. B. Huang and L. S. Zheng, *CrystEngComm*, 2011, **13**, 1591; (*h*) H. Y. Liu, H. Wu, J. Yang, Y. Y. Liu, B. Liu, Y. Y. Liu and J. F. Ma, *Cryst. Growth Des*., 2011, **11**, 2920; (*i*) A. B. Lago, R. Carballo, S. Rodriguez-Hermida and E. M. Vazquez-Lopez, *CrystEngComm*, 2013, **15**, 1563; (*j*) Y. H. Tan, J. J. Wu, H. Y. Zhou, L. F. Yang and B. H. Ye, *CrystEngComm*, 2012, **14**, 8117; (*k*) K. P. Rao, M. Higuchi, J. G. Duan and S. Kitagawa, *Cryst. Growth Des.*, 2013, **13**, 981.

14 (*a*) M. Wriedt, A. A. Yakovenko, G. J. Haider, A. V. Prosvirin, K. R. Dunbar and H. C. Zhou, *J. Am. Chem. Soc*., 2013, **135**, 4040; (*b*) C. P. Li and M. Du, *Chem. Commun*., 2011, **47**, 5958; (*c*) F. Y. Yi and Z. M. Sun, *Cryst. Growth Des*., 2012, **12**, 5693;(*d*) B. Li, R. J. Wei, J. Tao, R. B. Huang, L. S. Zheng and Z. P. Zheng, *J. Am. Chem. Soc*., 2010, **132**, 1558; (*e*) M. F. Wang, X. J. Hong, Q. G. Zhan, H. G. Jin, Y. T. Liu, Z. P. Zheng, S. H. Xu and Y. P. Cai, *Dalton Trans*., 2012, **41**, 11898; (*f*) X. M. Lin, H. C. Fang, Z. Y. Zhou, L. Chen, J. W. Zhao, S. Z. Zhu and Y. P. Cai, *CrystEngComm*, 2009, **11**, 847; (*g*) B. Liu, L. Y. Pang, L. Hou, Y. Y.Wang, Y. Zhang and Q. Z. Shi, *CrystEngComm*, 2012, **14**, 6246; (*h*) X. Zhu, X. G. Liu, B. L. Li and Y. Zhang, *CrystEngComm*, 2009, **11**, 997; (*i*) X. L. Zhao, L. L. Zhang, H. Q. Ma, D. Sun, D. X. Wang, S. Y. Feng and D. F. Sun, *RSC Adv*., 2012, **2**,

RSC Advances Accepted Manuscript

5543; (*j*) D. Sun, Y. H. Li, H. J. Hao, F. J. Liu, Y. M. Wen, R. B. Huang and L. S. Zheng, *Cryst. Growth Des*., 2011, **11**, 3323; (*k*) L. Wen, P. Cheng and W. B. Lin, *Chem. Commun*., 2012, **48**, 2846.

15 (*a*) Q. Y. Zhu, L. Yu, Y. R. Qin, L. B. Huo, M. Y. Shao and J. Dai, *CrystEngComm*, 2011, **13**, 2521; (*b*) B. Notash, N. Safari and H. R. Khavasi, *Inorg. Chem*., 2010, **49**, 11415; (*c*) J. K. Sun, P. Wang, Q. X. Yao, Y. J. Chen, Z. H. Li, Y. F. Zhang, L. M. Wu and J. Zhang, *J. Mater. Chem*., 2012, **22**, 12212; (*d*) Z. P. Deng, H. L. Qi, L. H. Huo, H. Zhao and S. Gao, *CrystEngComm*, 2011, **13**, 6632; (*e*) U. P. Singh, S. Kashyap, H. J. Singh and R. J. Butcher, *CrystEngComm*, 2011, **13**, 4110; (*f*) D. A. Safin, M. G. Babashkina, K. Robeyns and Y. Garcia, *Dalton Trans*., 2012, **41**, 4324; (g) X. H. Yan, Z. H. Cai, C. L. Yi, W. S. Liu, M. Y. Tan and Y. Tang, *Inorg. Chem.*, 2011, **50**, 2346; (*h*) I. H. Park, H. J. Kim and S. S. Lee, *CrystEngComm*, 2012, **14**, 4589; (*i*) S. H. Zhang, L. F. Ma, H. H. Zou, Y. G. Wang, H. Liang and M. H. Zeng, *Dalton Trans*., 2011, **40**, 11402; (*j*) Y. H. Lau, J. R. Price, M. H. Todd and P. J. Rutledge, *Chem. -Eur. J.*, 2011, **17**, 2850; (*k*) F. J. Liu, D. Sun, H. J. Hao, R. B. Huang and L. S. Zheng, *Cryst. Growth Des*., 2012, **12**, 354; (*l*) G. X. Liu, H. Xu, H. Zhou, S. Nishiharab and X. M. Ren, *CrystEngComm*, 2012, **14**, 1856.

16 (*a*) S. L. Cai, M. Pan, S. R. Zheng, J. B. Tan, J. Fan and W. G. Zhang, *CrystEngComm*, 2012, **14**, 2308; (*b*) P. Manna, S. K. Seth, A. Das, J. Hemming, R. Prendergast, M. Helliwell, S. R. Choudhury, A. Frontera and S. Mukhopadhyay, *Inorg. Chem*., 2012, **51**, 3557; (*c*) J. Yang, J. F. Ma, Y. Y. Liu, J.

RSC Advances Accepted Manuscript

C. Ma and S. R. Batten, *Inorg. Chem*., 2007, **46**, 6542; (*d*) R. Feng, F. L. Jiang, L. Chen, C. F. Yan, M. Y. Wu and M. C. Hong, *Chem. Commun*., 2009, 5296; (*e*) J. L. Gulbransen and C. M. Fitchett, *CrystEngComm*, 2012, **14**, 5394; (*f*) J. Chen, C. P. Li and M. Du, *CrystEngComm*, 2011, **13**, 1885; (*g*) F. Jin, H. Z. Wang, Y. Zhang, Y. Wang, J. Zhang, L. Kong, F. Y. Hao, J. X. Yang, J. Y. Wu, Y. P. Tian and H. P. Zhou, *CrystEngComm*, 2013, **15**, 3687.

17 (*a*) C. L. Zhang, M. D. Zhang, L. Qin and H. G. Zheng, *Cryst. Growth Des.*, 2014, **14**, 491; (*b*) M. L. Han, Y. P. Duan, D. S. Li, H. B. Wang, J. Zhao and Y. Y. Wang, *Dalton Trans*., 2014, **43**, 15450; (*c*) L. L. Han, X. Y. Zhang, J. S. Chen, Z. H. Li, D. F. Sun, X. P. Wang and D. Sun, *Cryst. Growth Des*., 2014, **14**, 2230; (*d*) L. N. Jin, Q. Liu and W. Y. Sun, *CrystEngComm*, 2014, **16**, 3816; (*e*) Y. F. Han, X. Y. Li, L. Q. Li, C. L. Ma, Z. Shen, Y. Song and X. Z. You, *Inorg. Chem*., 2010, **49**, 10781; (*f*) L. L. Liu, J. M. Du, Y. Y. Liu, F. Zhao and F. J. Ma, *J. Coord. Chem*., 2014, **67**, 136; (*g*) W. Wei, H. T. Yu, F. L. Jiang, B. Liu, J. Ma and M. C. Hong, *CrystEngComm*, 2012, **14**, 1693; (*h*) X. P. Yang, C. Chan, D. Lam, D. Schipper, J. M. Stanley, X. Y. Chen, R. A. Jones, B. J. Holliday, W. K. Wong, S. C. Chen and Q. Chen, *Dalton Trans*., 2012, **41**, 11449.

18 (*a*) Y. P. Li, Y. Chai, G. P. Yang, H. H. Miao, L. Cui, Y. Y. Wang and Q. Z. Shi, *Dalton Trans*., 2014, **43**, 10947; (*b*) X. L. Sun, Z. J. Wang, S. Q. Zang, W. C. Song and C. X. Du, *Cryst. Growth Des*., 2012, **12**, 4431; (*c*) L. L. Liu, C. X. Yu, Y. Zhou, J. Sun, P. P. Meng, D. Liu and R. J. Sa, *Inorg. Chem. Commun*., 2014, **40**, 194; (*d*) X. H. Chang, L. F. Ma, H. Guo and L. Y. Wang, *Cryst. Growth Des*.,

RSC Advances Accepted Manuscript

2012, **12**, 3638; (*e*) Y. Yang, P. Du, Y. Y. Liu and J. F. Ma, *Cryst. Growth Des*., 2013, **13**, 4781; (*f*) T. Liu, S. N. Wang, J. Lu, J. M. Dou, M. J. Niu, D. H. Lia and J. F. Bai, *CrystEngComm*, 2013, **15**, 5467; (*g*) L. F. Ma, L. Y. Wang, Y. Y. Wang, S. R. Batten and J. G. Wang, *Inorg. Chem*., 2009, **48**, 915; (*h*) L. Pan, B. Parker, X. Y. Huang, D. H. Oison, J. Y. Lee and J Li, *J. Am. Chem. Soc.*, 2006, **128**, 4180.

19 (*a*) F. Guo, B. Zhu, M. Liu, X. Zhang, J. Zhang and J. Zhao, *CrystEngComm*, 2013, **15**, 6191; (*b*) L. Zhang, J. Guo, Q. Meng, R. Wang and D. Sun, *CrystEngComm*, 2013, **15**, 9578; (*c*) L. Fan, X. Zhang, W. Zhang, Y. Ding, W. Fan, L. Sun, Y. Pang and X. Zhao, *Dalton Trans*., 2014, **43**, 6701; (*d*) B. Liu, L. Wei, N. N. Li, W. P. Wu, H. Miao, Y. Y. Wang and Q. Z. Shi, *Cryst. Growth Des*., 2014, **14**, 1110; (*e*) X. Zhang, L. Fan, W. Zhang, W. Fan, L. Sun and X. Zhao, *CrystEngComm*, 2014, **16**, 3203.

20 (a) S. L. Xiao, L. Liu, P. J. Ma and G. H. Cui, *Z. Anorg. Allg. Chem.*, 2014, **640**, 1484; (*b*) J. M. Hao, Y. N. Zhao, B. Y. Yu, K. V. Hecke and G. H. Cui, *Transition Met. Chem.*, 2014, **39**,741; (*c*) G. H. Cui, J. R. J. L. Tian, X. H. Bu and S. R. Batten, *Cryst. Growth Des.* 2005, **5**, 1775; (*d*) Y. Qi, F. Luo, S. R. Batten, Y. X. Che and J. M. Zheng, *Cryst. Growth Des.* 2008, **8**, 2806; (*e*) Y. Qi, F. Luo, Y. X. Che and J. M. Zheng, *Cryst. Growth Des.* 2008, **8**, 606; (*f*) J. H. Qin, L. F. Ma, Y. Hu and L. Y. Wang, *CrystEngComm*, 2012, **14**, 2891.

21 (*a*) J. Fan and B. E. Hanson, *Chem. Commun.*, 2005, 2327; (*b*) Y. H. So, *Macromolecules*, 1992, **25**, 516.

22 *SAINT, Version 6.02a*; Bruker AXS Inc., Madison, W1, 2002.

RSC Advances Accepted Manuscript

23 G. M. Sheldrick, *SADABS, Program for Bruker Area Detector Absorption Correction,* University of Göttingen, Göttingen, Germany, 1997.

24 (*a*) G. M. Sheldrick, S*HELXS-97, Program for Crystal Structure Solution*, University of Göttingen, Göttingen, Germany, 1997; (*b*) G. M. Sheldrick, S*HELXL-97, Program for Crystal Structure Refinement*, University of Göttingen, Göttingen, Germany, 1997.

25 (*a*) K. Nakamoto, *Infrared and Raman Spectra of Inorganic and Coordinated Compounds*, 5th edn, Wiley & Sons, New York, 1997; (*b*) C. G. Wang, Y. H. Xing, Z. P. Li, J. Li, X. Q. Zeng, M. F. Ge and S. Y. Niu, *Cryst. Growth Des.*, 2009, **9**, 1525; (*c*) R. S. Zhou, X. B. Cui, J. F. Song, X. Y. Xu, J. Q. Xu and T. G. Wang, *J. Solid State Chem*. 2008, **181**, 1565.

26 A. L. Spek, *J. Appl. Crystallogr*., 2003, **36**, 7.

27 (*a*) V. A. Blatov, *IUCr CompComm Newslett*., 2006, **7**, 4; (*b*) V. A. Blatov, *TOPOS, A Multipurpose Crystallochemical Analysis with the Program Package*, Samara State University, Russia, 2009.

28 (*a*) J. P. Sauvage, *Acc. Chem. Res*., 1998, **31**, 611; (*b*) C. Qin, X. L. Wang, E. B. Wang and Z. M. Su, *Inorg. Chem*., 2005, **44**, 7122; (*c*) B. F. Abrahams, M. G. Haywood and R. Robson, *CrystEngComm*, 2005, **7**, 629; (*d*) F. C. Liu, Y. F. Zeng, J. Jiao, X. H. Bu, J. Ribas and S. R. Batten, *Inorg. Chem*., 2006, **45**, 2776.

29 (*a*) N. Zhao, Y. E. Deng, P. Liu, C. X. An, T. X. Wang and Z. X. Lian, *Polyhedron*, 2015, **85**, 607; (*b*) L. M. Fan, X. T. Zhang, W. Zhang, Y. S. Ding, W. L. Fan, L. M. Sun, Y. Pang and X. Zhao, *Dalton Trans*., 2014, **43**, 6701; (*c*) R. M. Han, J. F. Ma,

RSC Advances Accepted Manuscript

776 Y. Y. Liu and J. Yang, *CrystengComm*, 2013, **15**, 5641; (*d*) K. K. Bisht and E.
777 Suresh, *Inorg. Chem.*, 2012, **51**, 9577; (*e*) B. K. Tripuramallu, P. Manna, S. N.
778 Reddy and S. K. Das, *Cryst. Growth Des.*, 2012, **12**, 777.
779 30 (*a*) C. Wang, T. Zhang and W. Lin, *Chem. Rev*., 2012, **112**, 1084; (*b*) Y. T. Wang,
780 H. H. Fan, H. Z. Wang and X. M. Chen, *Inorg. Chem*., 2005, **44**, 4148; (*c*) Y. T.
781 Wang, H. H. Fan, H. Z. Wang and X. M. Chen, *J. Mol. Struct*., 2005, **740**, 61; (*d*)
782 Y. T. Wang, M. L. Tong, H. H. Fan, H. Z. Wang and X. M. Chen, *Dalton Trans.*,
783 2005, 424; (*e*) Q. Ye, Y. Z. Tang, X. S. Wang and R. G. Xiong, *Dalton Trans.*,
784 2005, 1570; (*f*) D. W. Fu, W. Zhang and R. G. Xiong, *Cryst. Growth Des.*, 2008, **8**,
785 3461; (*g*) D. W. Fu, W. Zhang and R. G. Xiong, *Dalton Trans*., 2008, 3946.
786 31 S. K. Kurtz and T. T. Perry, *J. Appl. Phys*., 1968, **39**, 3798.
787 32 (*a*) D. W. Fu, Y. M. Song, G. X. Wang, Q. Ye, R. G. Xiong, T. Akutagawa, T.
788 Nakamura, P. W. H. Chan and S. D. Huang, *J. Am. Chem. Soc*., 2007, **129**, 5346;
789 (*b*) T. Okubo, R. Kawajiri, T. Mitani and T. Shimoda, *J. Am. Chem. Soc*., 2005,
790 **127**, 17598; (*c*) T. Sivakurnar, H. Y. Chang, J. Baek and P. S. Halasyamani, *Chem.*
791 *Mater.*, 2007, **19**, 4710; (*d*) D. L. deMurillas, R. Pinol, M. B. Ros, J. L. Serrano, T.
792 Sierra and M. R. delaFuente, *J. Mater. Chem*., 2004, **14**, 1117.
793 33 (*a*) L. Song, S. W. Du, J. D. Lin, H. Zhou, T. Li, *Cryst. Growth Des*., 2007, **7**,
794 2268; (*b*) X. Q. Liang, J. T. Jia, T. Wu, D. P. Li, L. Liu, Tsolmon and G. S. Zhu,
795 *CrystEngComm*, 2010, **12**, 3499; (*c*) Z. Su, M. S. Chen, J. Fan, M. Chen, S. S.
796 Chen, L. Luo and W. Y. Sun, *CrystEngComm*, 2010, **12**, 2040.

RSC Advances Accepted Manuscript

34 (*a*) Q. Ye, Y. M. Song, G. X. Wang, K. Chen, D. W. Fu, P. W. H. Chan, J. S. Zhu, S. D. Huang and R. G. Xiong, *J. Am. Chem. Soc*., 2006, **128**, 6554; (*b*) H. Y. Ye, D. W. Fu, Y. Zhang, W. Zhang, R. G. Xiong and S. P. Huang, *J. Am. Chem. Soc*., 2009, **131**, 42.

35 (*a*) J. H. Wang, G. M. Tang, T. X. Qin, S. C. Yan, Y. T. Wang, Y. Z. Cui and S. W. Ng, *J. Solid State Chem.*, 2014, **219**, 55; (*b*) F. L. Du, H. B. Zhang, C. B. Tian and S. W. Du, *Cryst. Growth Des.*, 2013, **13**, 1736; (*c*) Y. Z. Tang, M. Zhou, J. Huang, Y. H. Tan, J. S. Wu and H. R. Wen, *Inorg. Chem.*, 2013, **52**, 1779; (*d*) Y. H. Liu, C. C. Peng, S. H. Lee, P. H. Chien and P. C. Wu, *CrystEngComm.*, 2013, **15**, 10333.

RSC Advances Accepted Manuscript

807 **Table 1** X-ray crystallographic data for complexes **1** - **7**

Complex	**1**	**2**	**3**
Formula	$C_{29}H_{34}N_6O_7Ni$	$C_{56}H_{54}N_8O_{13}Ni_2$	$C_{30}H_{27}BrN_6O_6NiZn$
Formula weight	637.33	1164.49	771.57
Temperature (K)	293(2)	293(2)	293(2)
Crystal system	Orthorhombic	Triclinic	Cubic
Space group	$Pna2_1$	P-1	$P2_13$
a (Å)	18.023(3)	10.1090(14)	14.6382(4)
b (Å)	11.862(2)	11.2544(16)	14.6382(4)
c (Å)	13.824(3)	12.3282(17)	14.6382(4)
α (º)	90	70.576	90
β (º)	90	77.903	90
γ (º)	90	82.210	90
V (Å^3)	2955.4(9)	1290.1(3)	3136.63(15)
Z	4	1	4
D_{calc} (Mg/m^3)	1.432	1.499	1.634
μ (mm^{-1})	0.713	0.806	2.691
F(000)	1336	606	1560
θ range (º)	2.06-25.50	1.92-25.10	1.97-25.48
Reflections collected	14704	6473	22244
Independent reflections (R_{int})	5377 (0.0563)	4500 (0.0663)	1966 (0.0818)
Data/restraints/parameters	5377 / 1 / 391	4500 / 4 / 371	1966 / 13 / 137
Goodness-of-fit	1.070	1.004	1.044
R indices [$I > 2\sigma(I)$][a,b]	R_1 = 0.0573	R_1 = 0.0413	R_1 = 0.0380
	wR_2 = 0.1225	wR_2 = 0.1097	wR_2 = 0.0828
R indices (all data)	R_1 = 0.0703	R_1 = 0.0474	R_1 = 0.0545
	wR_2 = 0.1284	wR_2 = 0.1120	wR_2 = 0.0899

808 [a] $R_1 = \Sigma||F_o| - |F_c||/\Sigma|F_o|$.

809 [b] $wR_2 = |\Sigma w(|F_o|^2 - |F_c|^2)|/\Sigma|w(F_o)^2|^{1/2}$

810

RSC Advances Accepted Manuscript

Complex	**4**	**5**
Formula	$C_{33}H_{38}N_6O_5Ni$	$C_{33}H_{35}N_6O_5Ni$
Formula weight	657.40	654.38
Temperature (K)	293(2)	293(2)
Crystal system	Orthorhombic	Triclinic
Space group	$P2_12_12_1$	P-1
a (Å)	10.5786(6)	8.9712(9)
b (Å)	15.8768(8)	10.0571(10)
c (Å)	18.6358(11)	18.3348(19)
α (º)	90	74.5820(10)
β (º)	90	79.4070(10)
γ (º)	90	83.0710(10)
V (Å^3)	3130.0(3)	1563.0(3)
Z	4	2
D_{calc} (Mg/m^3)	1.395	1.390
μ (mm^{-1})	0.671	0.672
F(000)	1384	686
θ range (º)	2.21-25.10	2.14-25.50
Reflections collected	12615	11104
Independent reflections (R_{int})	5336 (0.0224)	5738 (0.0434)
Data/restraints/parameters	5336 / 2 / 408	5738 / 2 / 409
Goodness-of-fit	1.057	1.065
R indices [$I > 2\sigma(I)$][a,b]	R_1 = 0.0381	R_1 = 0.0509
	wR_2 = 0.1050	wR_2 = 0.1029
R indices (all data)	R_1 = 0.0415	R_1 = 0.0785
	wR_2 = 0.1081	wR_2 = 0.1180

811 [a] $R_1 = \Sigma||F_o| - |F_c||/\Sigma|F_o|$.

812 [b] $wR_2 = |\Sigma w(|F_o|^2 - |F_c|^2)|/\Sigma|w(F_o)^2|^{1/2}$

813

RSC Advances Accepted Manuscript

Complex	**6**	**7**
Formula	$C_{26}H_{30}N_4O_6Ni$	$C_{26}H_{28}N_4O_5Ni$
Formula weight	553.25	535.23
Temperature (K)	293(2)	293(2)
Crystal system	Triclinic	Triclinic
Space group	*P*-1	*P*-1
a (Å)	9.0020(5)	10.2427(9)
b (Å)	10.2280(6)	11.0898(10)
c (Å)	14.9680(9)	11.8660(10)
α (º)	78.7850(10)	105.9120(10)
β (º)	84.2210(10)	94.2520(10)
γ (º)	78.2830(10)	106.0960(10)
V (Å^3)	1320.97(13)	1228.84(19)
Z	2	2
D_{calc} (Mg/m^3)	1.391	1.447
μ (mm^{-1})	0.781	0.835
F(000)	580	560
θ range (º)	2.07-25.10	2.25-25.50
Reflections collected	16100	9751
Independent reflections (R_{int})	4680 (0.1024)	4560 (0.0201)
Data/restraints/parameters	4680 / 2 / 345	4560 / 2 / 318
Goodness-of-fit	1.055	1.041
R indices [$I > 2\sigma(I)$][a,b]	$R_1 = 0.0420$	$R_1 = 0.0421$
	$wR_2 = 0.1131$	$wR_2 = 0.1071$
R indices (all data)	$R_1 = 0.0528$	$R_1 = 0.0477$
	$wR_2 = 0.1450$	$wR_2 = 0.1109$

[a] $R_1 = \Sigma||F_o| - |F_c||/\Sigma|F_o|$.

[b] $wR_2 = |\Sigma w(|F_o|^2 - |F_c|^2)|/\Sigma|w(F_o)^2|^{1/2}$

RSC Advances Accepted Manuscript

Captions for Scheme and Figures:

Scheme 1 Structures of imidazole-containing ligands and polycarboxylates used in this work.

Fig. 1 (a) Coordination environment of Ni(II) ions in **1** with the ellipsoids drawn at the 30% probability level; hydrogen atoms and water molecules were omitted for clarity. Symmetry codes: A -x+3/2, y-1/2, z-1/2; B x-1/2, -y-1/2, z; C x, y-1, z. (b) Ball-stick representation of the Ni-titmb sheet in **1**. (c) Schematic representation of the 2D (6,3) framework. (d) Stick representation of a 3D structure of **1** along the *c*-axis. (e) Schematic view of the $(6^3)(6^9.8)$ topology.

Fig. 2 (a) Coordination environment of Ni(II) ions in **2** with the ellipsoids drawn at the 30% probability level; hydrogen atoms were omitted for clarity. Symmetry codes: A x-1, y, z; B x+1, y, z+1. (b) Molecular packing of the sub-layer in **2**. (c)The square-like network of **2**. Only the nickel atoms and the connections between them are shown. The orientation of the diagram is along *a*-axis. (d)View of the 3D hydrogen-bonding network in the packing of **2** along the *c* axis; O–H···O interactions are shown as dashed lines.

Fig. 3 (a) Coordination environment of Ni(II) and Zn(II) ions in **3** with the ellipsoids drawn at the 30% probability level; hydrogen atoms were omitted for clarity. Symmetry codes: A y, z, x; B z, x, y; C y, z, x; D z, x, y. (b) Heterometallic binuclear $ZnNi(CO_2)_3Br$ unit observed for **3**. (c) Schematic representation of the (10,3)-a net in **3** along the *c*-axis; the binuclear units are represented by the green balls and the BTC^{3-} anions are represented by the blue nods. (d) Schematic representation of the second

RSC Advances Accepted Manuscript

(10,3)-a net in **3** along the *c*-axis; the binuclear units are represented by the purple balls and the titmb ligands are represented by the yellow nods. (e) Schematic representation of the overall network topology in complex **3**; titmb and BTC^{3-} ligands are represented by yellow and blue nods, respectively.

Fig. 4 (a) Coordination environment of Ni(II) ions in **4** with the ellipsoids drawn at the 30% probability level; hydrogen atoms and water molecules were omitted for clarity. Symmetry codes: A -x+1, y-1/2, -z+1/2; 2; B -x, y+1/2, -z+1/2; C -x+1, y+1/2, -z+1/. (b) Ball-stick representation of the Ni-titmb sheet in **4**. (c) Schematic representation of the 2D (6,3) framework. (d) Stick representation of a 3D structure of **4** along the *c*-axis. (e) Schematic view of the $(3.5^2)(3^2.5^3.6^4.7)$ topology.

Fig. 5 (a) Coordination environment of Ni(II) ions in **5** with the ellipsoids drawn at the 30% probability level; hydrogen atoms and water molecules were omitted for clarity. Symmetry codes: A x, y-1, z; B -x, 2-y, 2-z; C -1-x, 1-y, 1-z; D 1-x, 2-y, 1-z. (b) View of the 1D chain of Ni(II) linked by $TBDC^{2-}$ anion in **5**. (c) View of the (6, 3) layer of Ni(II) bridged by bix ligands; (d) View of the 3D framework with $(4^6.6^4)$-**bnn** hexagonal BN topology. (e) Schematic illustration of the two-fold interpenetration network in **5**.

Fig. 6 (a) Coordination environment of Ni(II) ions in **6** with the ellipsoids drawn at the 30% probability level; hydrogen atoms were omitted for clarity. Symmetry codes: A x, y-1, z; B x+1, y-1, z. (b)View of 2D layer constructed by Ni(II) ions, TBDC anions, and mbix ligands. (c) Schematic representation of topology of **6** (the green spheres represent the Ni(II) ions and blue and purple lines represent the mbix ligands

RSC Advances Accepted Manuscript

862 and TBDC anions, respectively). (d)The 3D supramolecular network constructed by
863 π–π interactions in **6**.

864 **Fig. 7** (a) Coordination environments of the Ni(II) atoms in **7** with the ellipsoids
865 drawn at the 30% probability level; hydrogen atoms were omitted for clarity.
866 Symmetry codes: A x+1, y ,z; B -x+1, -y+1, -z. (b) View of 24-membered $[Ni_2(obix)_2]$
867 ring in **7**. (c) Schematic representation of the 1D tubular structure in **7**.

868 **Fig. 8** TGA curves of complexes **1** – **7**.

869 **Fig. 9** Electric hysteresis loops of complex **1** under different voltages at room
870 temperature.
871

RSC Advances Accepted Manuscript

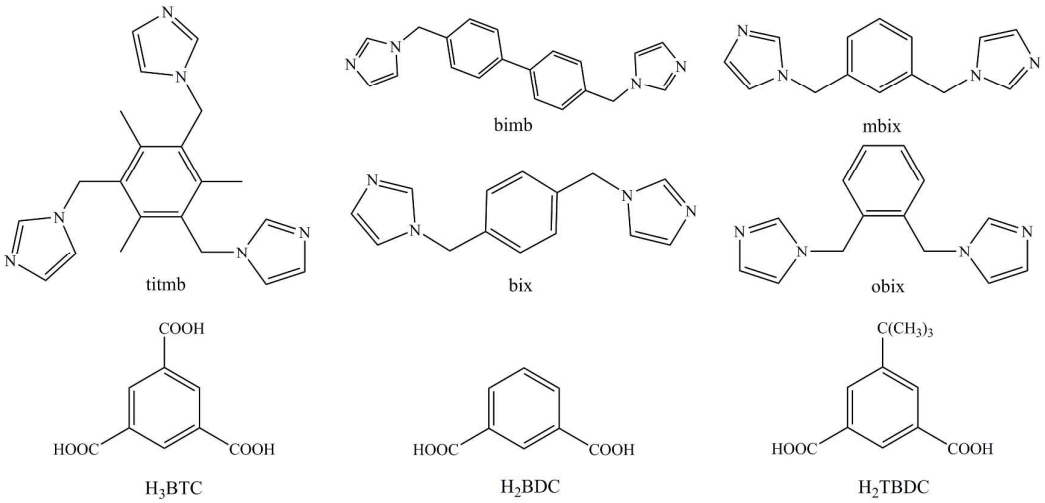

872
873
874 Scheme 1
875

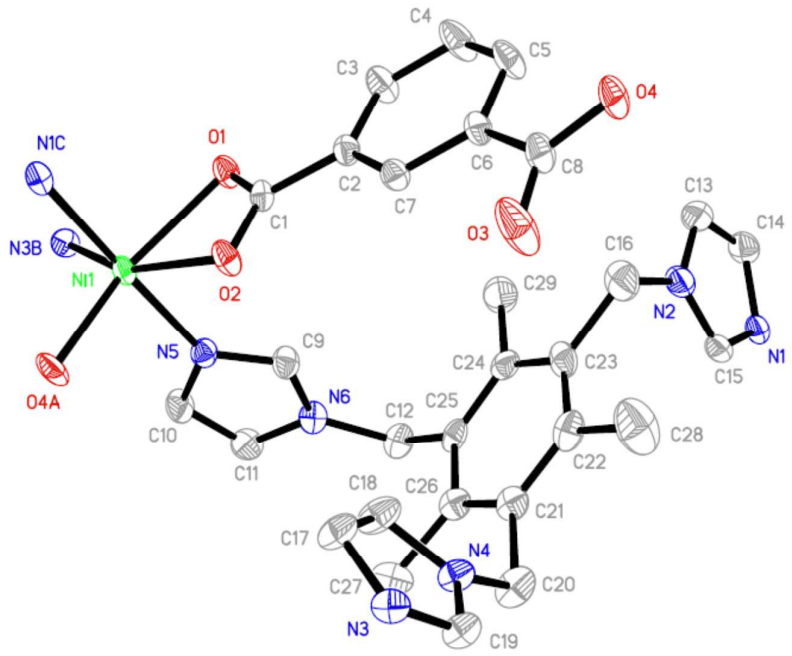

876
877 (a)

RSC Advances Accepted Manuscript

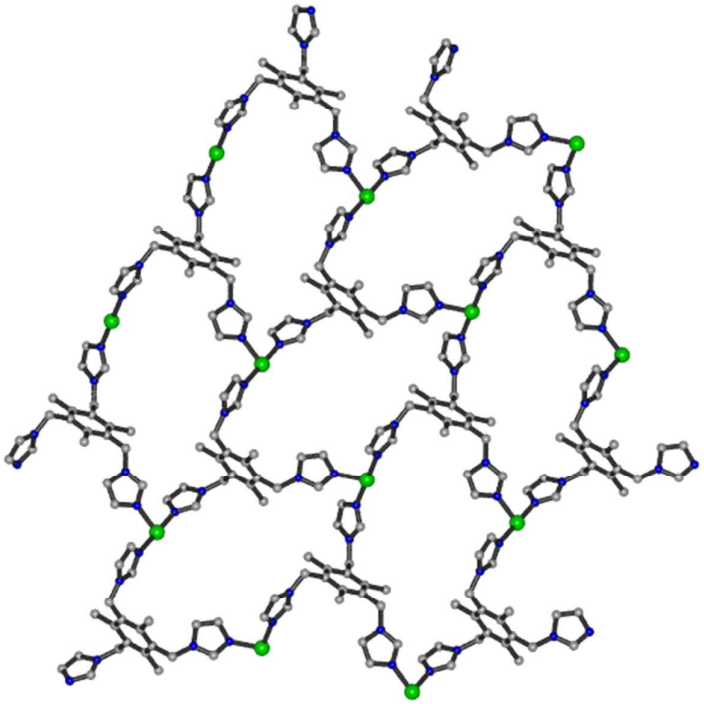

878
879 (b)

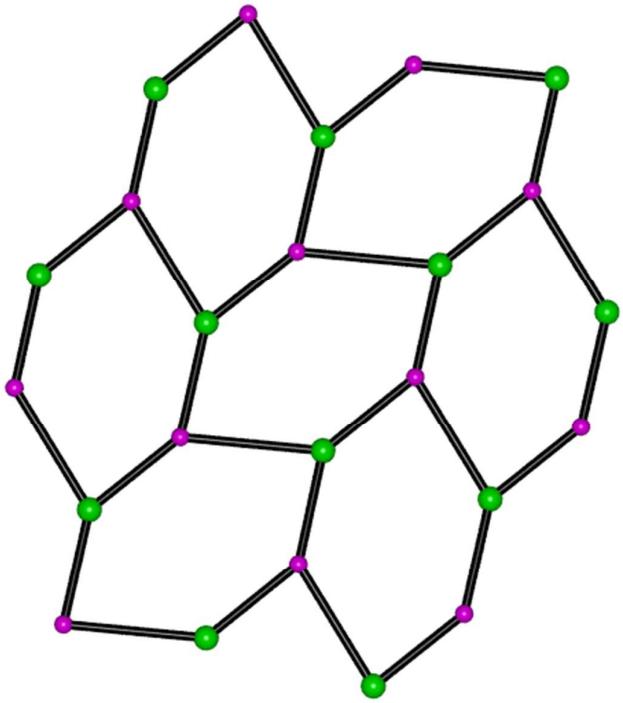

880
881 (c)

RSC Advances Accepted Manuscript

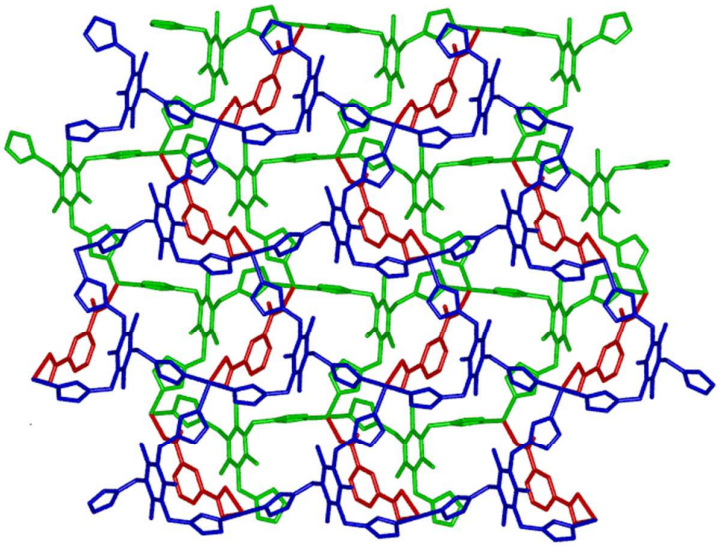

(d)

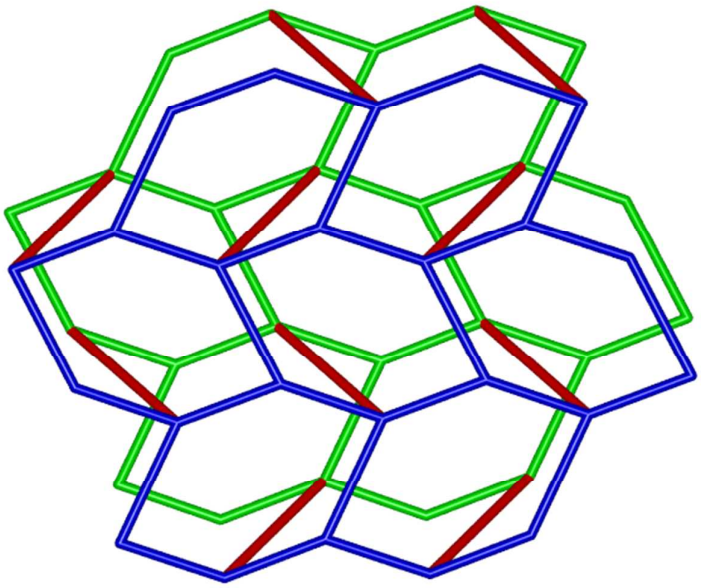

(e)

Figure 1.

RSC Advances Accepted Manuscript

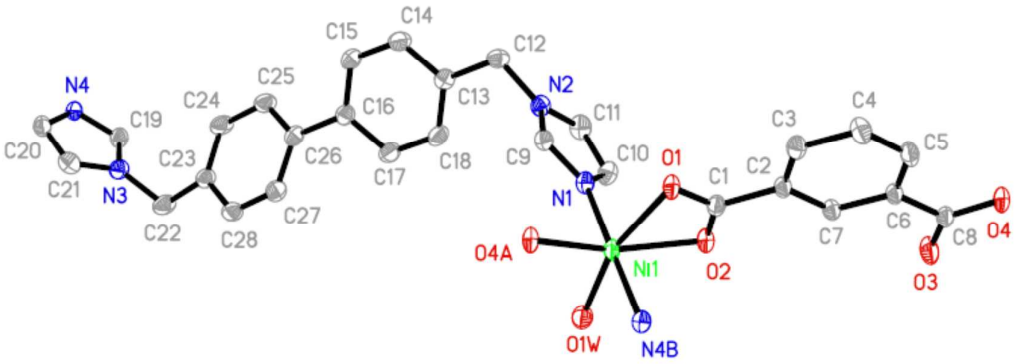

888

889 (a)

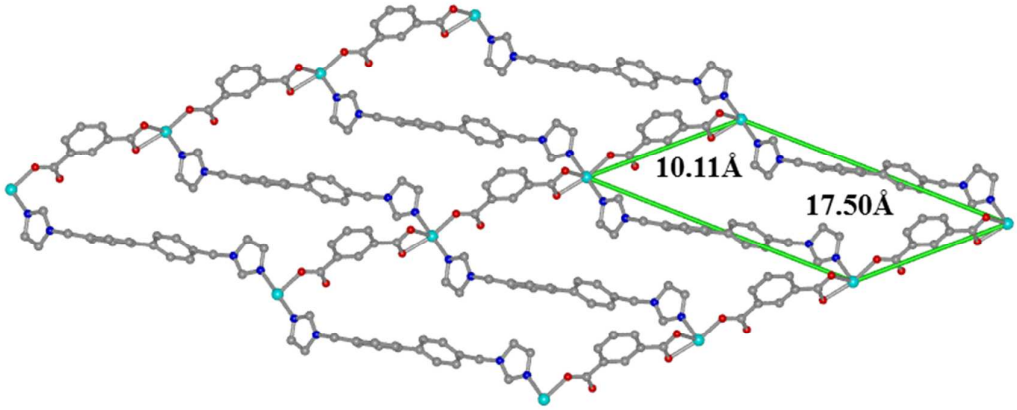

890

891 (b)

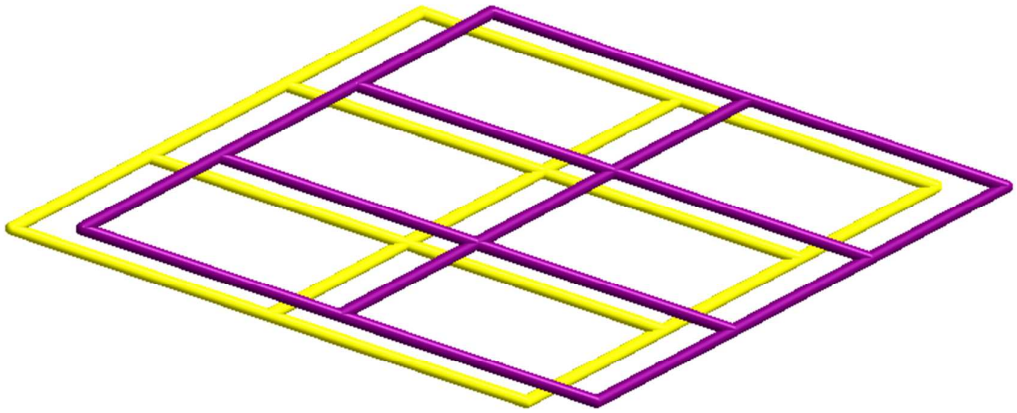

892

893 (c)

RSC Advances Accepted Manuscript

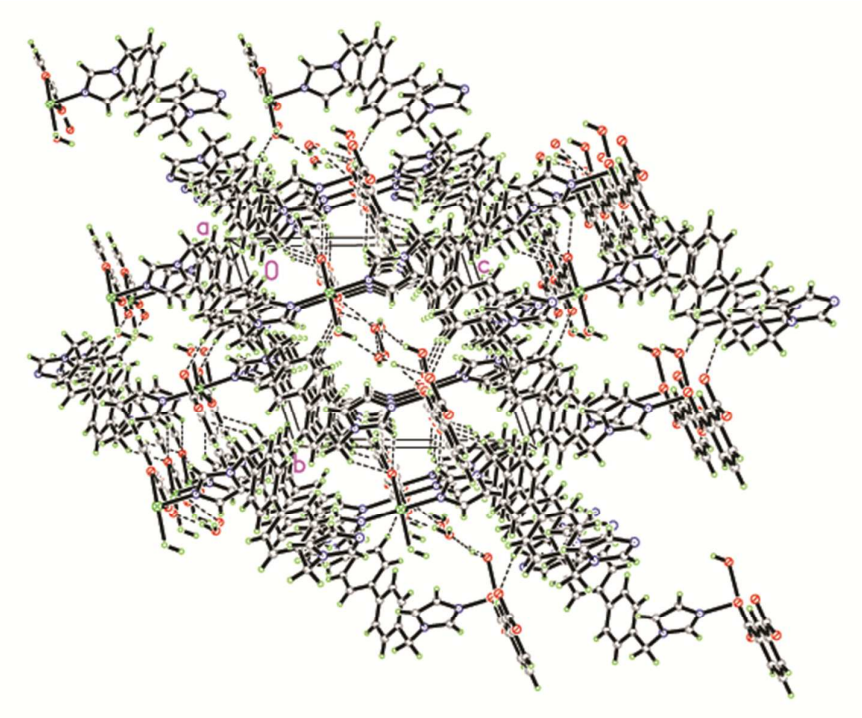

(d)

Figure 2.

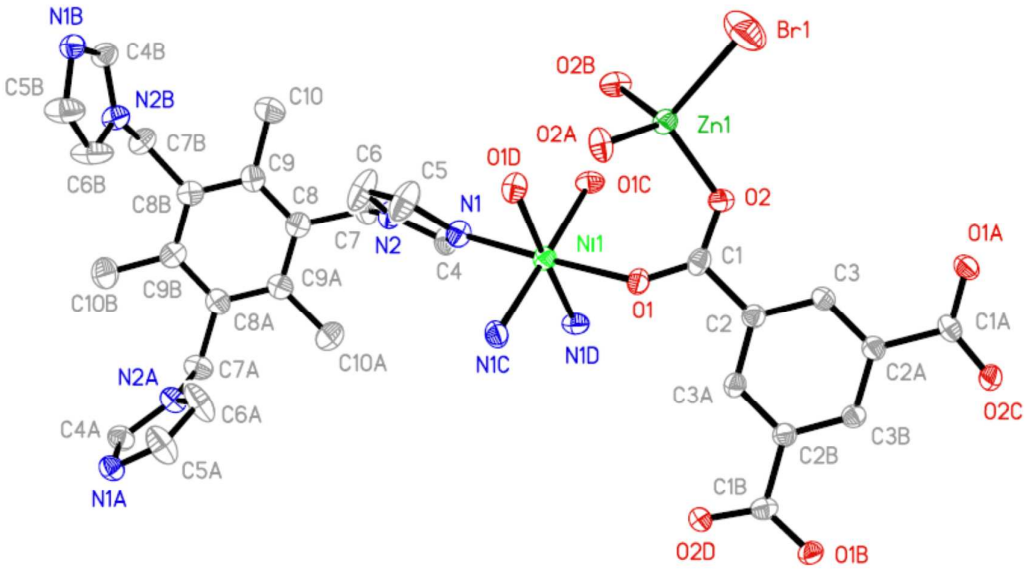

(a)

RSC Advances Accepted Manuscript

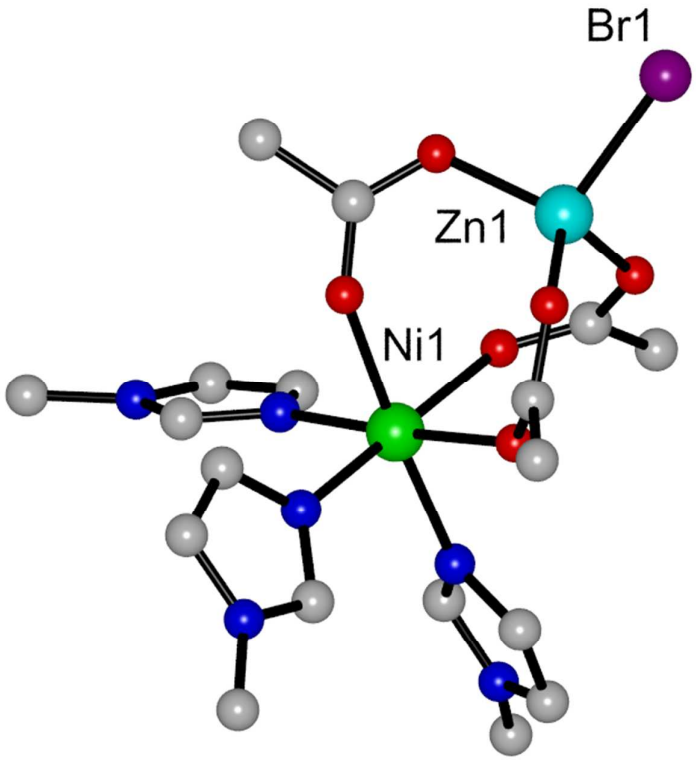

899
900 (b)

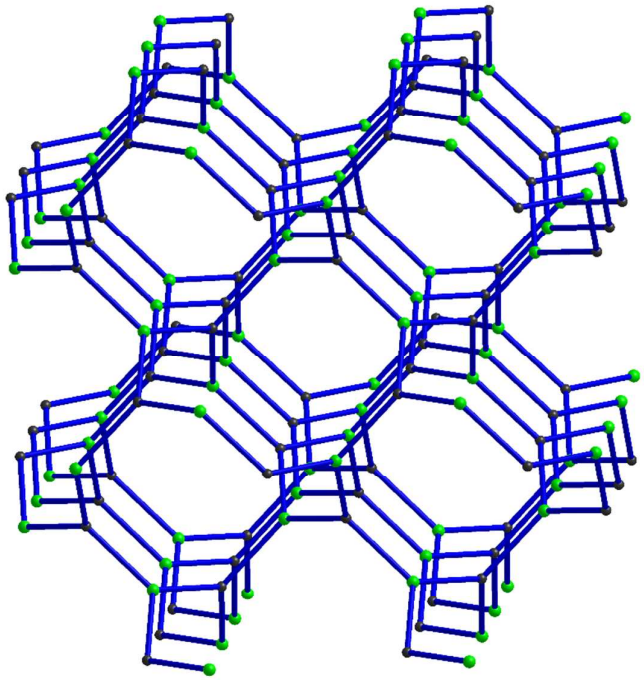

901
902 (c)

RSC Advances Accepted Manuscript

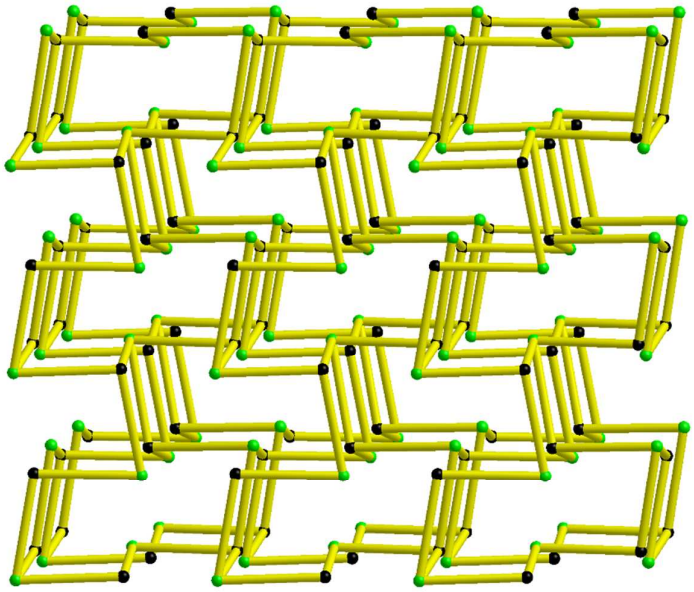

(d)

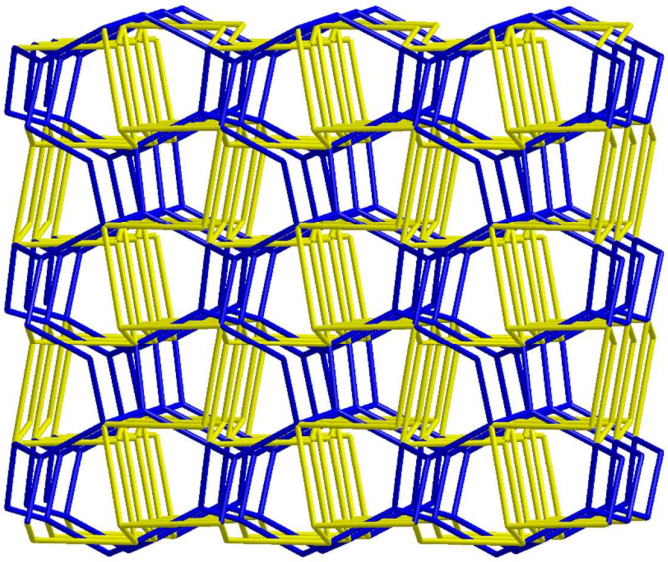

(e)

Figure 3.

RSC Advances Accepted Manuscript

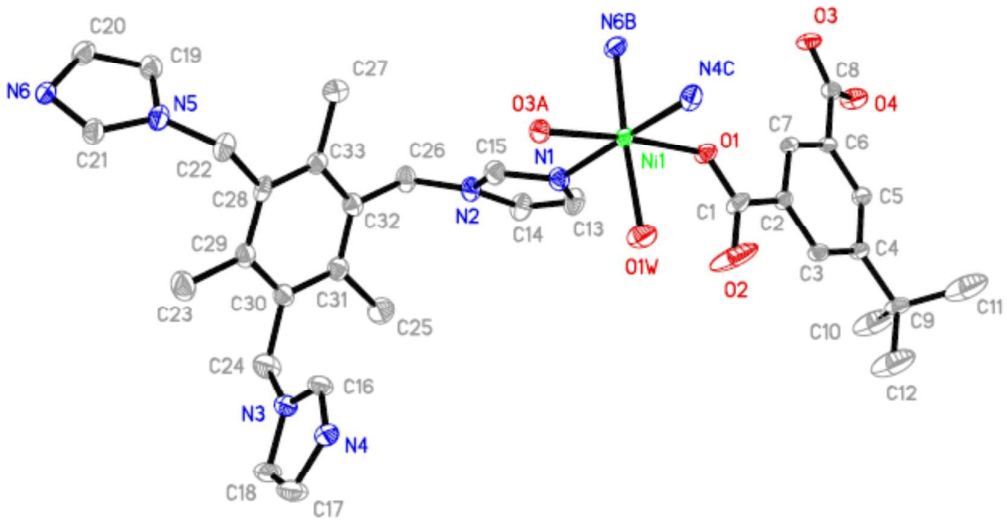

908

909 (a)

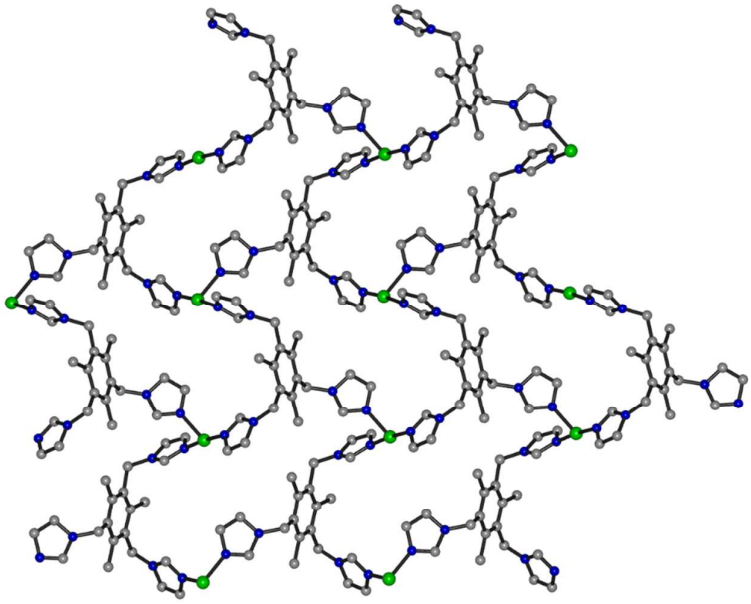

910

911 (b)

RSC Advances Accepted Manuscript

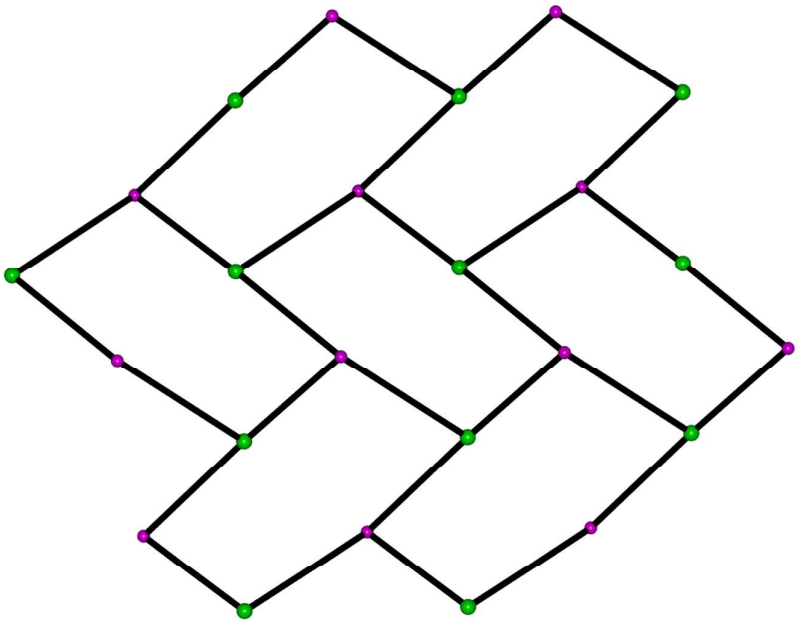

912

913 (c)

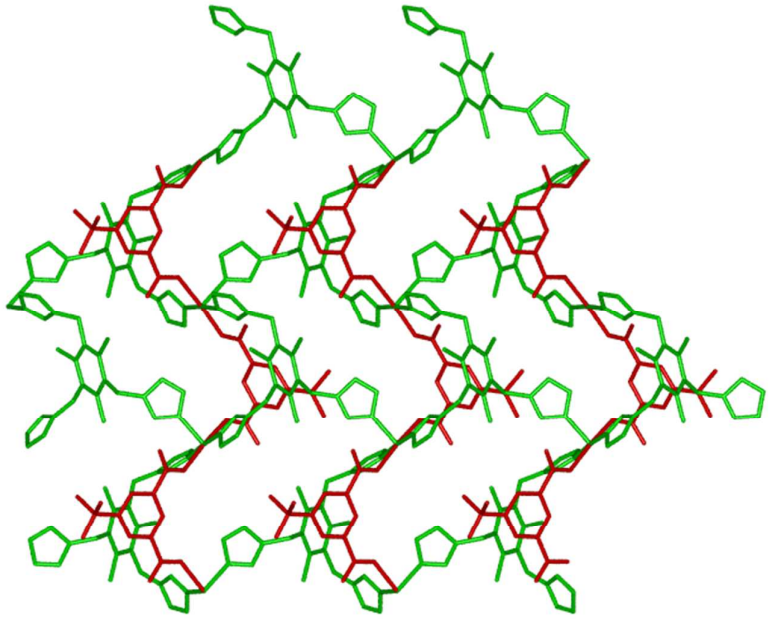

914

915 (d)

RSC Advances Accepted Manuscript

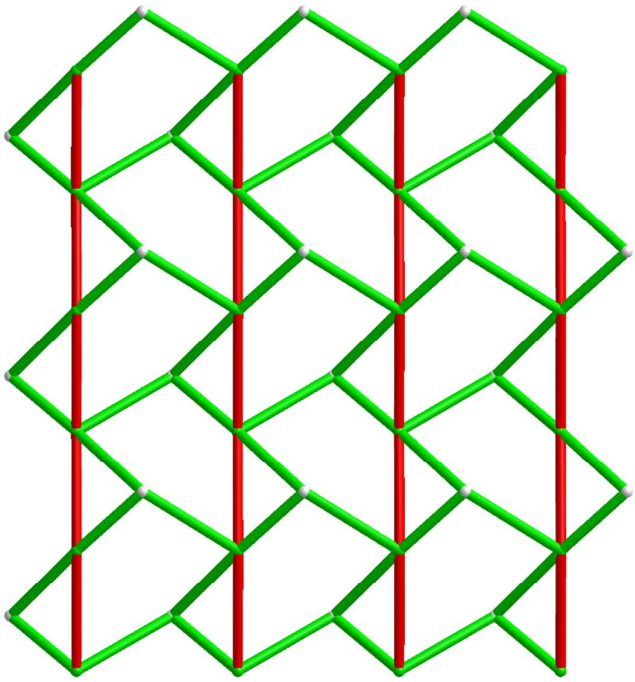

916

917 (e)

918 Figure 4.

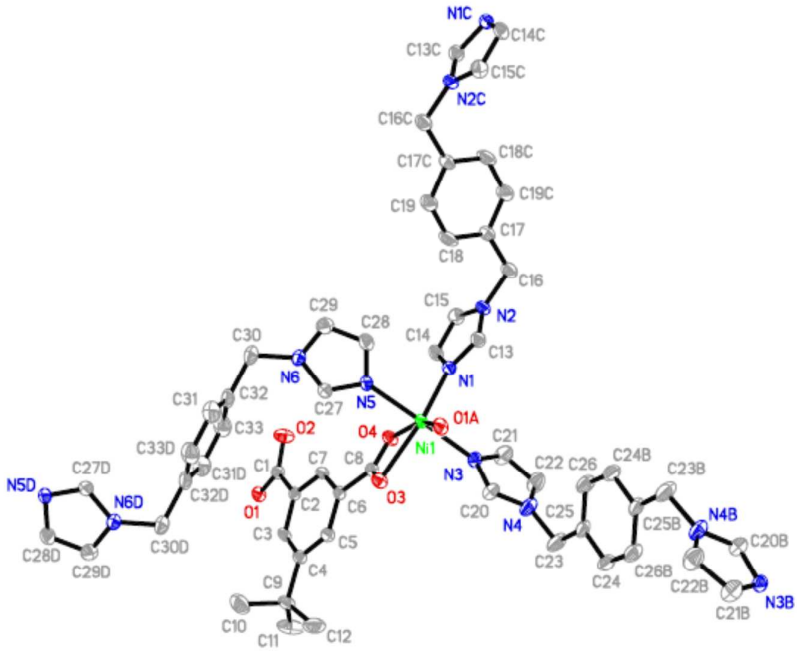

919

920 (a)

RSC Advances Accepted Manuscript

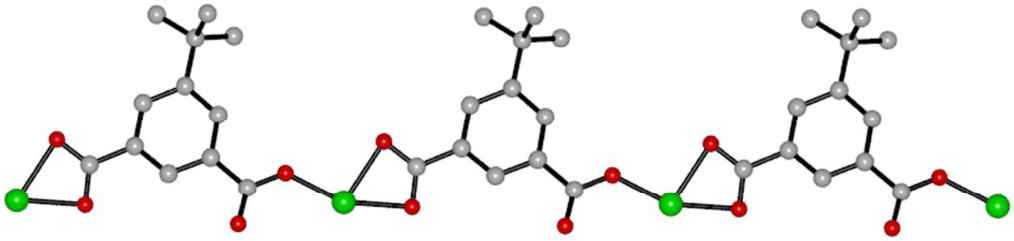

(b)

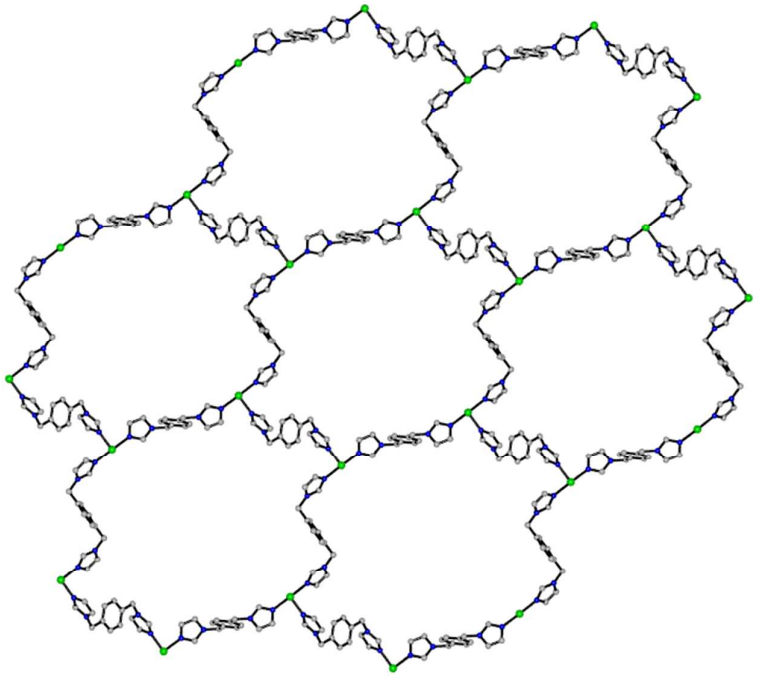

(c)

RSC Advances Accepted Manuscript

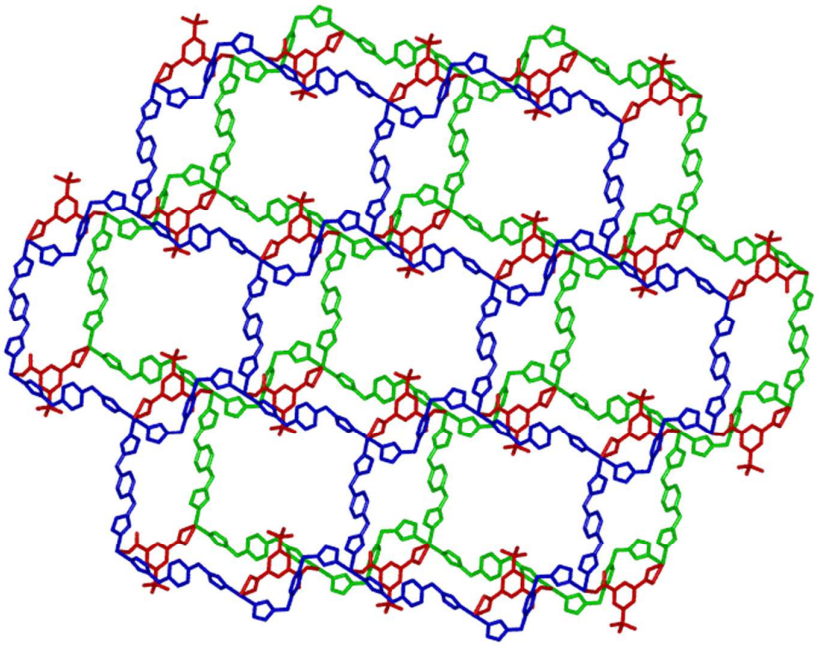

(d)

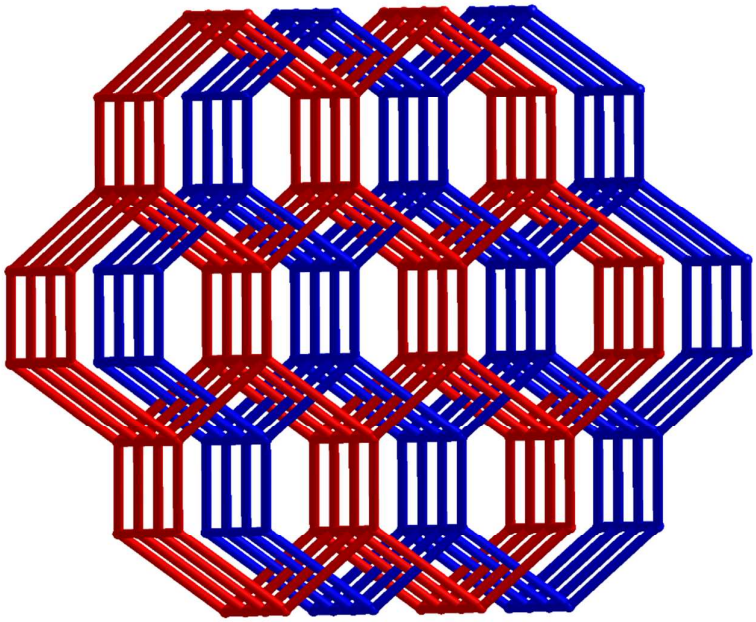

(e)

Figure 5.

RSC Advances Accepted Manuscript

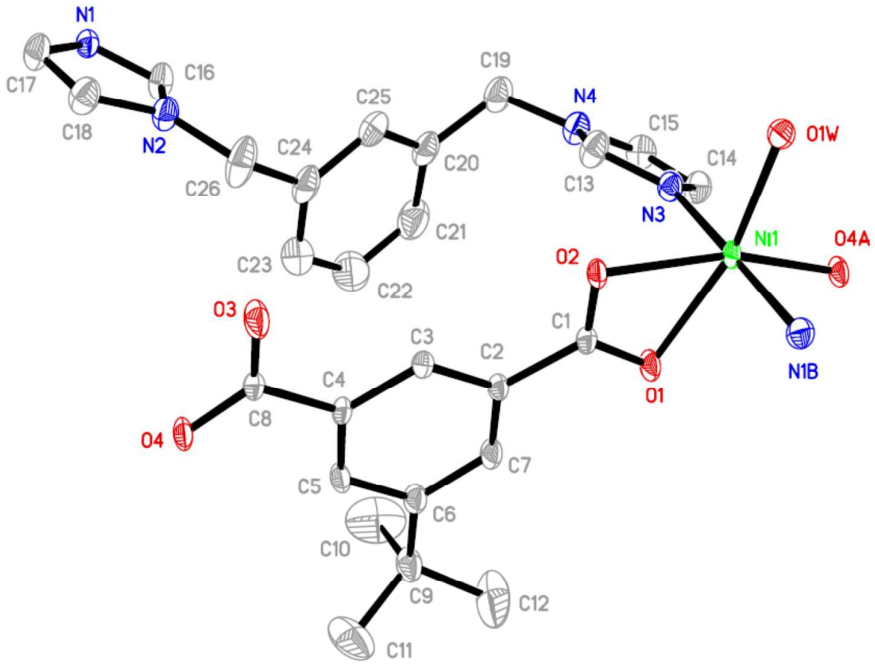

930

931 (a)

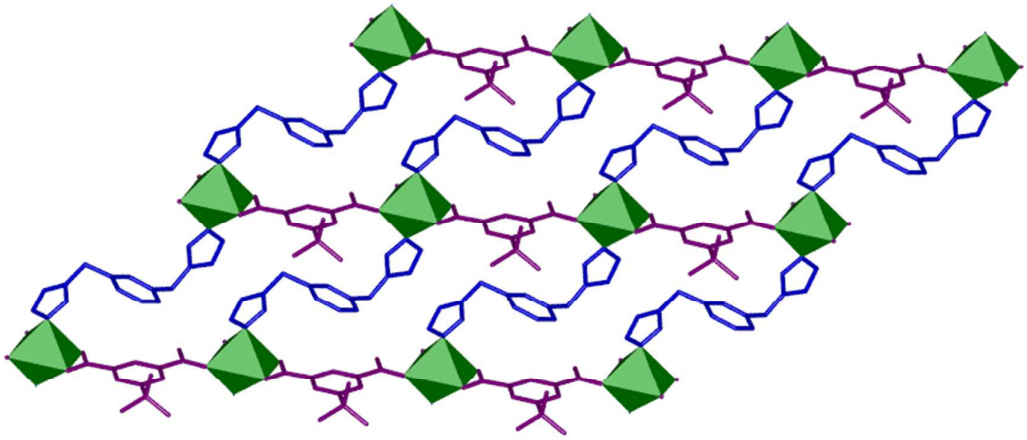

932

933 (b)

RSC Advances Accepted Manuscript

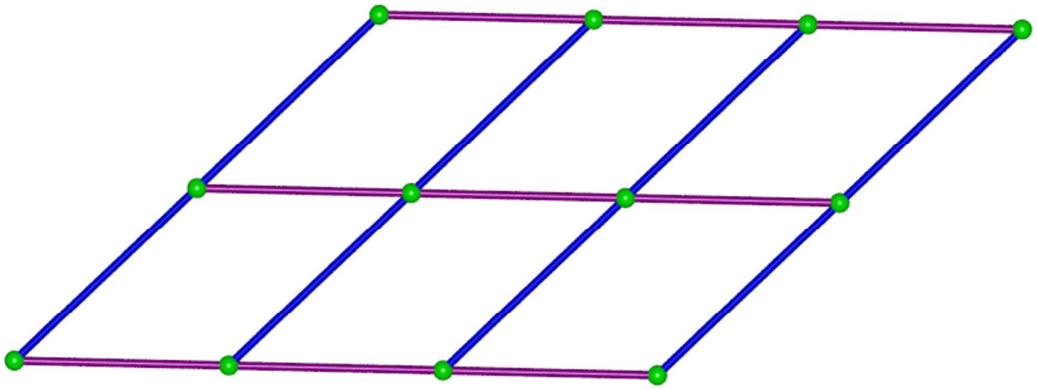

(c)

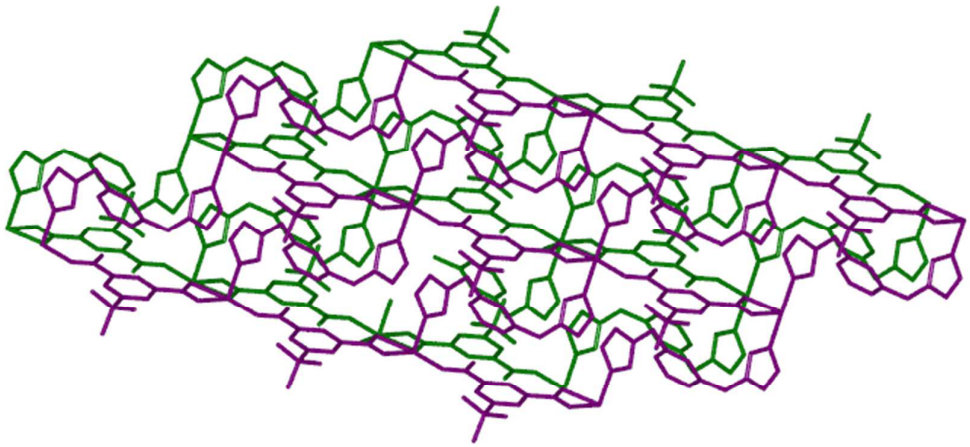

(d)

Figure 6.

RSC Advances Accepted Manuscript

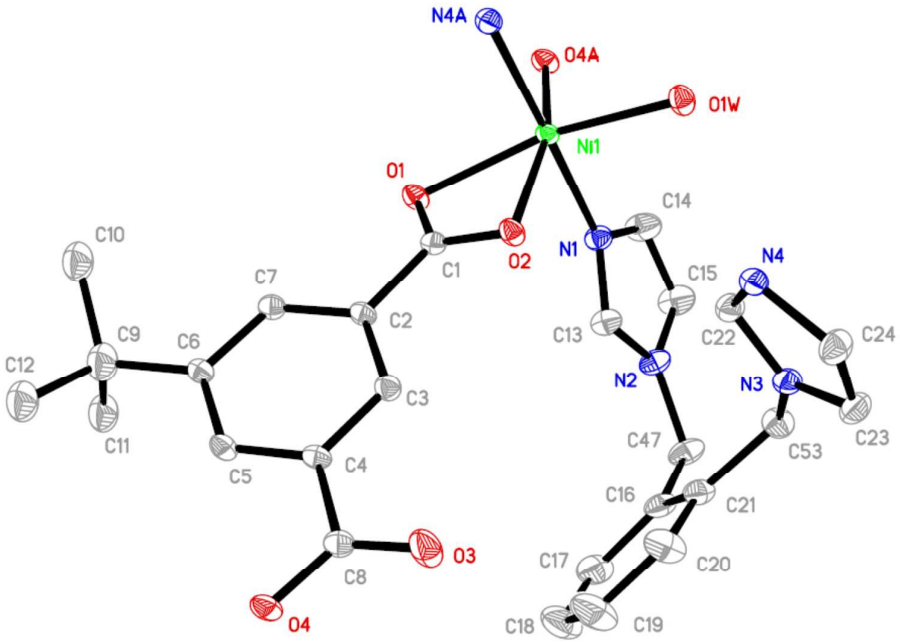

939

940 (a)

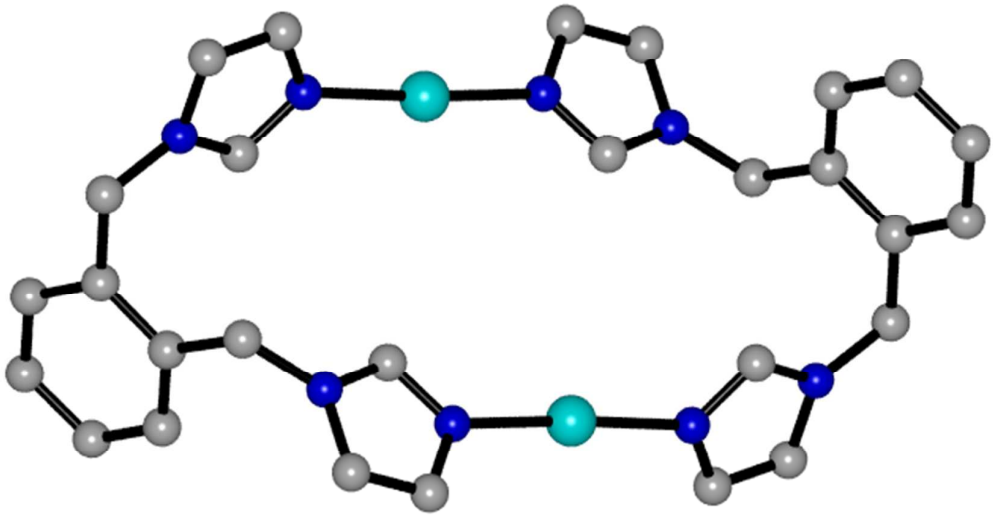

941

942 (b)

RSC Advances Accepted Manuscript

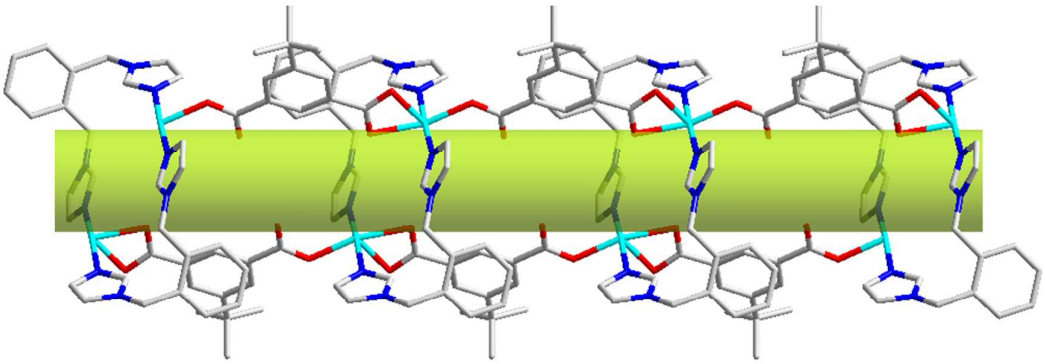

(c)

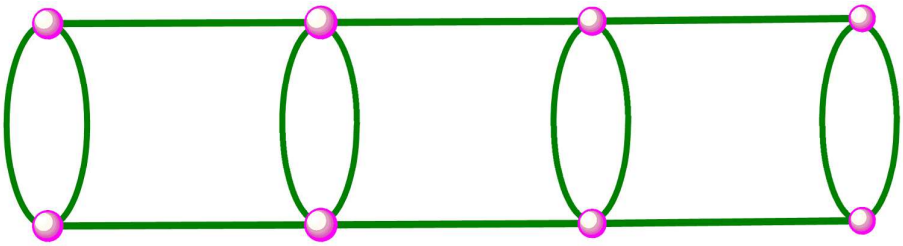

(d)

Figure 7.

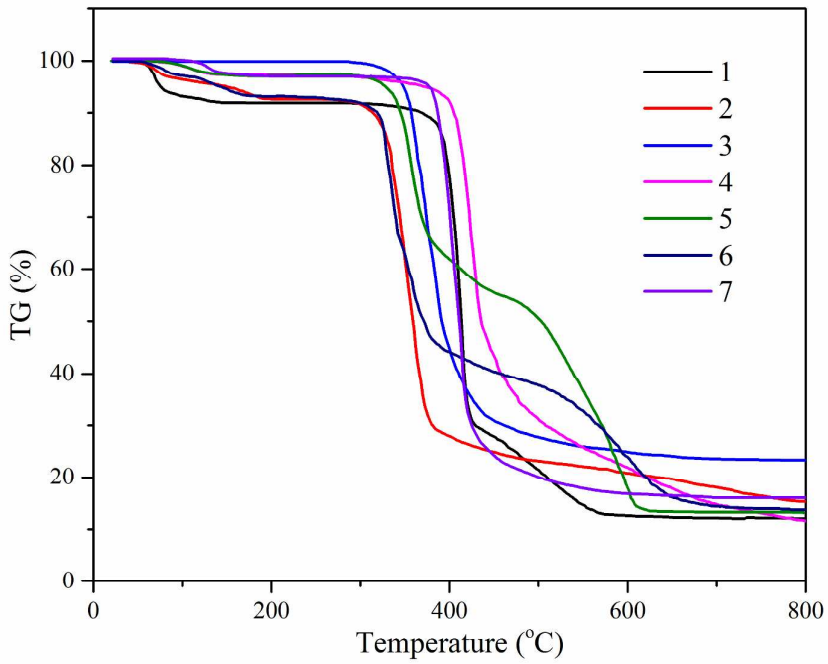

Figure 8.

RSC Advances Accepted Manuscript

950

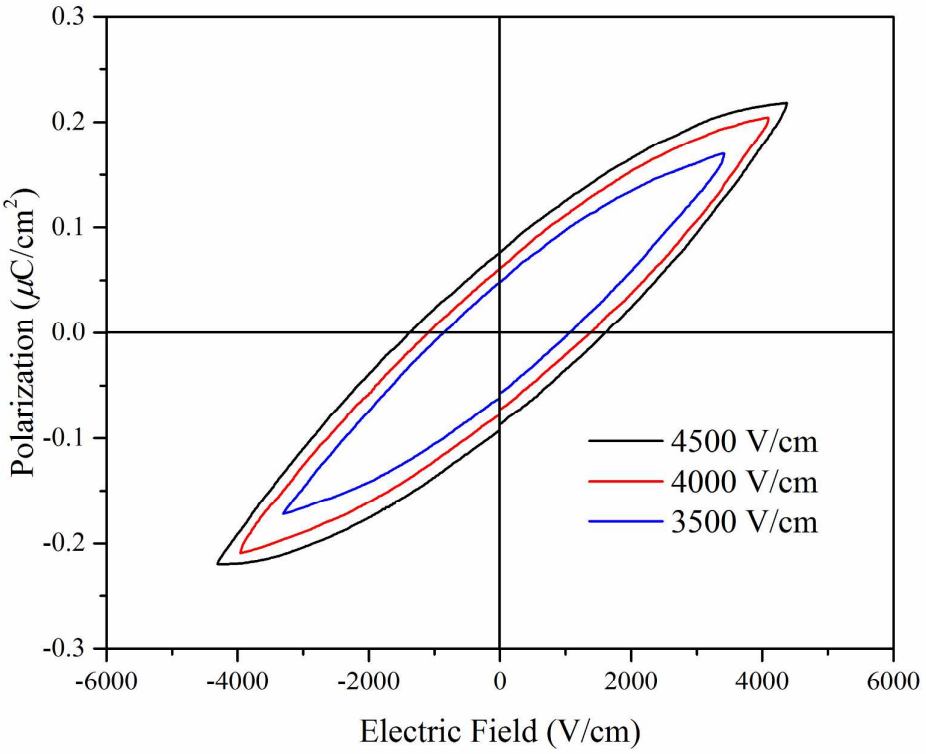

951

952 Figure 9.

RSC Advances Accepted Manuscript

***Graphical Abstract*:**

Seven nickel(II) coordination polymers, based on varied polycarboxylates and different imidazole-containing ligands, are obtained, indicating that the different species of functional groups, the number and position of the carboxylic groups in the carboxylates as well as the auxiliary ligands have crucial influences on the final structures.

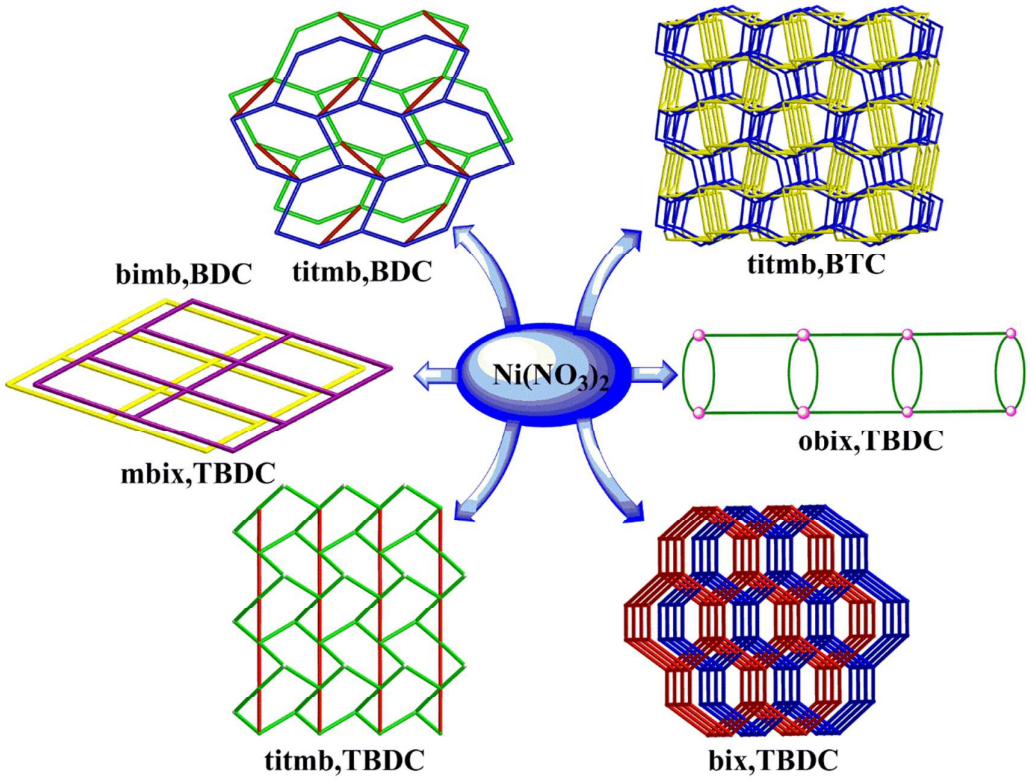

RSC Advances Accepted Manuscript